Summer Fellowship Report

On

Renewable Energy Integration of 37-Bus System Using OpenModelica & OpenIPSL

Submitted by

Mohd Ayaz

Under the guidance of

Prof. Kannan M.Moudgalya
Chemical Engineering Department
IIT Bombay

Acknowledgement

I would like to thank **Prof. Kannan Moudgalya** , Professor, Department of Chemical Engineering, IIT Bombay for establishing this fellowship, which I believe was an excellent introduction to me on open-source software and technologies.

I would also like to thank my mentor **Mr. Syed Yasser Ali** for providing valuable insight and expertise, as well as assisting me in overcoming the several difficulties I faced during this project. Their advice on the modeling and simulation of the network significantly improved the accuracy of results. I would never be able to finish the project without their support. I am also grateful to **Ms. Usha Vishwanathan** for her kind support.

I would also like to show my gratitude to my fellow interns and peers, who were constantly there to clarify my doubts and recommend improvements to the project. Their help and support was of immense value to me.

Sincerely,

Mohd Ayaz

Contents

List of Tables

List of Figures

Chapter 1

Introduction

1.1 OpenModelica

OpenModelica is a free and open-source modelling environment that uses “Modelica" modelling language. It follows equation oriented approach. OpenModelica can be used for modelling, simulation, optimization and analysis of complex steady state and dynamic systems.

OpenModelica contains a very exhaustive library called Modelica Standard Library (MSL) which is a collection of different libraries from different domains such as electrical, mechanical, hydraulic, mathematics, etc.

OpenModelica complies expressions, equations, functions and algorithms into efficient C code. The generated C code is combined with a library of utility functions, a run-time library, and a numerical Differential-Algebric Equation (DAE) solver. OpenModelica Connection Editor, called as OMEdit is the integrated Graphical User Interface (GUI) in OpenModelica for graphical modelling and editing. OMEdit consists of several libraries for various domains like Electrical, Magnetic, Math, Thermal, etc. It provides various user friendly features like representation of a model in the form of block diagrams. OMEdit can be used for creating custom models and for editing or drawing connections between the model interfaces. It also allows users to plot graphs between parameters of the model simulated.

1.2 OpenIPSL

The OpenIPSL or Open-Instance Power System Library is library of power system component models written in the Modelica language that can be used for power system dynamic analysis, such as phasor time-domain simulations.

OpenIPSL is currently developed and maintained by Prof. Luigi Vanfretti's research group ALSETLab at Rensselaer Polytechnic Institute, Troy, NY .

The iPSL is a Modelica library developed during the iTesla project. The members of this project (OpenIPSL) at SmarTS Lab (now ALSETLab) where key developers of the iPSL until March 31, 2016, when the iTesla project was completed. Prof. Luigi Vanfretti lead the development of a large amount of the models of the library (particularly those that replicate results from PSAT and PSS/E). iPSL is part of the iTesla Tool, and thus, it is subject to the needs of the consortium that develops the iTesla Tool. Therefore, the SmarTS Lab / ALSETLab team decided to create the OpenIPSL fork in order to develop the library in a direction that is more suitable for researchers and teachers/professors, and in a transparent, open source software approach.

Chapter 2

Brief Description About Load Flow Studies

2.1 Introduction

Load flow studies are one of the most important aspects of power system planning and operation. The load flow gives us the sinusoidal steady state of the entire system - voltages, real and reactive power generated and absorbed and line losses.

Through the load flow studies we can obtain the voltage magnitudes and angles at each bus in the steady state. This is rather important as the magnitudes of the bus voltages are required to be held within a specified limit. Once the bus voltage magnitudes and their angles are computed using the load flow, the real and reactive power flow through each line can be computed. Also based on the difference between power flow in the sending and receiving ends, the losses in a particular line can also be computed. Furthermore, from the line flow we can also determine the over and under load conditions.

The steady state power and reactive power supplied by a bus in a power network are expressed in terms of nonlinear algebraic equations. We therefore would require iterative methods for solving these equations. In this chapter we shall discuss two of the load flow methods.

2.2 Real and Reactive Power

For the formulation of the real and reactive power entering a b us, we need to define the following quantities. Let the voltage at the i^{th} bus be denoted by

$$V_i = |V_i|\angle\delta_i = |V_i|(\cos\delta_i + j\sin\delta_i) \qquad (2.1)$$

Also let us define the self admittance at bus- i as

$$Y_{ii} = |Y_{ii}|\angle\theta_{ii} = |Y_{ii}|(\cos\theta_{ii} + j\sin\theta_{ii}) = G_{ii} + jB_{ii} \qquad (2.2)$$

Similarly the mutual admittance between the buses i and j can be written as

$$Y_{ij} = |Y_{ij}|\angle\theta_{ij} = |Y_{ij}|(\cos\theta_{ij} + j\sin\theta_{ij}) = G_{ij} + jB_{ij} \qquad (2.3)$$

Let the power system contains a total number of n buses. The current injected at bus- i is given as

$$I_i = Y_{i1}V_1 + Y_{i2}V_2 + \cdots + Y_{in}V_n$$
$$= \sum_{k=1}^{n} Y_{ik}V_k \tag{2.4}$$

It is to be noted we shall assume the current entering a bus to be positive and that leaving the bus to be negative. As a consequence the power and reactive power entering a bus will also be assumed to be positive. The complex power at bus- i is then given by

$$P_i - jQ_i = V_i^* I_i = V_i^* \sum_{k=1}^{n} Y_{ik}V_k \tag{2.5}$$

$$= |V_i|(\cos\delta_i - j\sin\delta_i)\sum_{k=1}^{n}|Y_{ik}V_k|\,(\cos\theta_{ik} + j\sin\theta_{ik})(\cos\delta_k + j\sin\delta_k)$$

$$= \sum_{k=1}^{n}|Y_{ik}V_iV_k|\,(\cos\delta_i - j\sin\delta_i)(\cos\theta_{ik} + j\sin\theta_{ik})(\cos\delta_k + j\sin\delta_k)$$

$$= \sum_{k=1}^{n}|Y_{ik}V_iV_k|\,(\cos\delta_i - j\sin\delta_i)[\cos(\theta_{ik} + \delta_k) + j\sin(\theta_{ik} + \delta_k)]$$

$$= \sum_{k=1}^{n}|Y_{ik}V_iV_k|\,[\cos(\theta_{ik} + \delta_k - \delta_i) + j\sin(\theta_{ik} + \delta_k - \delta_i)]$$

$$P_i - jQ_i = \sum_{k=1}^{n}|Y_{ik}V_iV_k|\cos(\theta_{ik} + \delta_k - \delta_i) + j\sum_{k=1}^{n}|Y_{ik}V_iV_k|\;\sin(\theta_{ik} + \delta_k - \delta_i)$$

By comparison :

$$P_i = \sum_{k=1}^{n}|Y_{ik}V_iV_k|\cos(\theta_{ik} + \delta_k - \delta_i) \tag{2.6}$$

$$Q_i = -\sum_{k=1}^{n}|Y_{ik}V_iV_k|\;\sin(\theta_{ik} + \delta_k - \delta_i) \tag{2.7}$$

2.3 Classification of Buses

For load flow studies it is assumed that the loads are constant and they are defined by their real and reactive power consumption. It is further assumed that the generator terminal voltages are tightly regulated and therefore are constant. The main objective of the load flow is to find the voltage magnitude of each bus and its angle when the powers generated and loads are pre-specified.

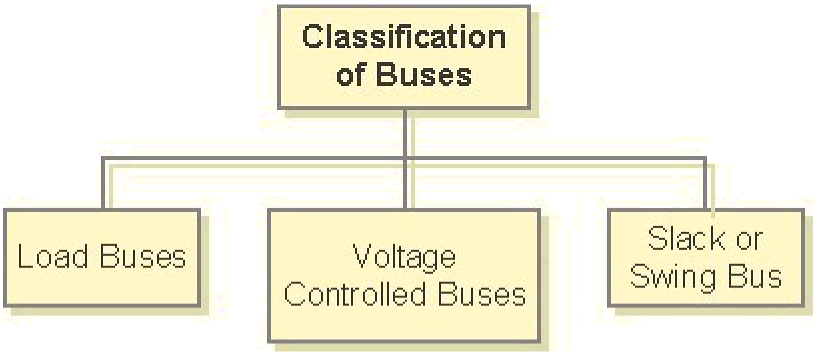

2.3.1 Load Bus

In these buses no generators are connected and hence the generated real power P_{Gi} and reactive power Q_{Gi} are taken as zero. The load drawn by these buses are defined by real power $-P_{Li}$ and reactive power $-Q_{Li}$ in which the negative sign accommodates for the power flowing out of the bus. This is why these buses are sometimes referred to as P-Q bus. The objective of the load flow is to find the bus voltage magnitude $|V_i|$ and its angle δ_i.

2.3.2 Voltage Controlled Buses / Generator Bus / P-V Bus

These are the buses where generators are connected. Therefore the power generation in such buses is controlled through a prime mover while the terminal voltage is controlled through the generator excitation. Keeping the input power constant through turbine-governor control and keeping the bus voltage constant using automatic voltage regulator, we can specify constant P_{Gi} and $| V_i |$ for these buses. This is why such buses are also referred to as P-V buses. It is to be noted that the reactive power supplied by the generator Q_{Gi} depends on the system configuration and cannot be specified in advance. Furthermore we have to find the unknown angle δ_i of the bus voltage.

2.3.3 Slack or Swing Bus

Usually this bus is numbered 1 for the load flow studies. This bus sets the angular reference for all the other buses. Since it is the angle difference between two voltage sources that dictates the real and reactive power flow between them, the particular angle of the slack bus is not important. However it sets the reference against which angles of all the other bus voltages are measured. For this reason the angle of this bus is usually chosen as 0° . Furthermore it is assumed that the magnitude of the voltage of this bus is known.

2.4 Methods of Load Flow Solution

There are three methods of load flow solution mentioned in this chapter.

2.4.1 Gauss-Seidel Method

The basic power flow equations (2.6) and (2.7) are nonlinear. In an n -bus power system, let the number of P-Q buses be n_p and the number of P-V (generator) buses be n_g such that $n = n_p + n_g + 1$. Both voltage magnitudes and angles of the P-Q buses and voltage angles of the P-V buses are unknown making a total number of $2n_p + n_g$ quantities to be determined. Amongst the known quantities are $2n_p$ numbers of real and reactive powers of the P-Q buses, $2n_g$ numbers of real powers and voltage magnitudes of the P-V buses and voltage magnitude and angle of the slack bus. Therefore there are sufficient numbers of known quantities to obtain a solution of the load flow problem. However, it is rather difficult to obtain a set of closed form equations from (2.6) and (2.7). We therefore have to resort to obtain iterative solutions of the load flow problem.

At the beginning of an iterative method, a set of values for the unknown quantities are chosen. These are then updated at each iteration. The process continues till errors between all the known and actual quantities reduce below a pre-specified value.

In the Gauss-Seidel load flow we denote the initial voltage of the i^{th} bus by $V_i^{(0)}$, $i = 2, \ldots, n$. This should read as the voltage of the i^{th} bus at the 0th iteration, or initial guess. Similarly this voltage after the first iteration will be denoted by $V_i^{(1)}$.

In this Gauss-Seidel load flow the load buses and voltage controlled buses are treated differently. However in both these type of buses we use the complex power equation given in (2.5) for updating the voltages. Knowing the real and reactive power injected at any bus we can expand (2.5) as

$$P_{i,inj} - jQ_{i,inj} = V_i^* \sum_{k=1}^{n} Y_{ik} V_k = V_i^* [Y_{i1}V_1 + Y_{i2}V_2 + \cdots + Y_{ii}V_i + \cdots + Y_{in}V_n] \tag{2.8}$$

We can written (2.8) as

$$V_i = \frac{1}{Y_{ii}} \left[\frac{P_{i,inj} - jQ_{i,inj}}{V_i^*} - Y_{i1}V_1 - Y_{i2}V_2 - \cdots - Y_{in}V_n \right] \tag{2.9}$$

- Updating Load Bus Voltages

$$V_i^{(k)} = \frac{1}{Y_{ii}} \left[\frac{P_{i,inj} - jQ_{i,inj}}{V_i^{*(k-1)}} - Y_{i1}V_1^{(k)} - Y_{i2}V_2^{(k)} - \cdots - Y_{in}V_n^{(k)} \right] \tag{2.10}$$

Where, k=1,2,3,…….,n (No. of iteration)

- Updating P-V Bus Voltages

$$Q_{i,inj} = -Im\left[V_i^* \sum_{k=1}^{n} Y_{ik} V_k\right]$$
$$= -Im[V_i^* \{Y_{i1}V_1 + Y_{i2}V_2 + \cdots + Y_{ii}V_i + \cdots + Y_{in}V_n\}] \quad (2.11)$$

For k^{th} iteration :

$$Q_{i,inj}^{(k)} = -Im\left[V_i^{*(k-1)}\left\{Y_{i1}V_1 + Y_{i2}V_2^{(k)} + \cdots + Y_{ii}V_i^{(k-1)} + \cdots + Y_{in}V_n^{(k-1)}\right\}\right] \quad (2.12)$$

Where, k=1,2,3,…….,n (No. of iteration)

Update Voltages :

$$V_i^{(k)} = \frac{1}{Y_{ii}}\left[\frac{P_{i,inj} - jQ_{i,inj}^{(k)}}{V_i^{*(k-1)}} - Y_{i1}V_1^{(k)} - Y_{i2}V_2^{(k)} - \cdots - Y_{in}V_n^{(k)}\right]$$

Where, k=1,2,3,…….,n (No. of iteration)

Sometimes to accelerate computation in the P-Q buses the voltages obtained from (4.12) is multiplied by a constant. The voltage update of bus- *i* is then given by

$$V_{i,acc}^{(k)} = (1-\lambda)V_{i,acc}^{(k-1)} + \lambda V_i^{(k)} = V_{i,acc}^{(k-1)} + \lambda\left\{V_i^{(k)} - V_{i,acc}^{(k-1)}\right\}$$

where λ is a constant that is known as the **acceleration factor** . The value of λ has to be below 2.0 for the convergence to occur.

2.4.2 Newton-Raphson Method

Let us assume that an n -bus power system contains a total n_p number of P-Q buses while the number of P-V (generator) buses be n_g such that $n = n_p + n_g + 1$. Bus-1 is assumed to be the slack bus. We shall further use the mismatch equations of ΔP_i and ΔQ_i . The approach to Newton-Raphson load flow is similar to that of solving a system of nonlinear equations using the **Newton-Raphson method** at each iteration we have to form a Jacobian matrix and solve for the corrections from an equation.

$$J\begin{bmatrix}\Delta\delta_2\\ \vdots\\ \Delta\delta_n\\ \dfrac{\Delta|V|_2}{|V|_2}\\ \vdots\\ \dfrac{\Delta\left|V_{1+n_0}\right|}{\left|V_{1+n_0}\right|}\end{bmatrix}=\begin{bmatrix}\Delta P_2\\ \vdots\\ \Delta P_n\\ \Delta Q_2\\ \vdots\\ \Delta Q_{1+n_0}\end{bmatrix} \tag{2.13}$$

Jacobian matrix is divided into submatrices as :

$$J=\begin{bmatrix}J_{11} & J_{12}\\ J_{21} & J_{22}\end{bmatrix} \tag{2.14}$$

The submatrices are :

$$J_{11}=\begin{bmatrix}\dfrac{\partial P_2}{\partial\delta_2} & \cdots & \dfrac{\partial P_2}{\partial\delta_n}\\ \vdots & \ddots & \vdots\\ \dfrac{\partial P_n}{\partial\delta_2} & \cdots & \dfrac{\partial P_n}{\partial\delta_n}\end{bmatrix} \tag{2.15}$$

$$J_{12}=\begin{bmatrix}|V_2|\dfrac{\partial P_2}{\partial|V_2|} & \cdots & \left|V_{1+n_0}\right|\dfrac{\partial P_2}{\partial\left|V_{1+n_0}\right|}\\ \vdots & \ddots & \vdots\\ |V_2|\dfrac{\partial P_2}{\partial|V_n|} & \cdots & \left|V_{1+n_0}\right|\dfrac{\partial P_n}{\partial\left|V_{1+n_0}\right|}\end{bmatrix} \tag{2.16}$$

$$J_{21}=\begin{bmatrix}\dfrac{\partial Q_2}{\partial\delta_2} & \cdots & \dfrac{\partial Q_2}{\partial\delta_n}\\ \vdots & \ddots & \vdots\\ \dfrac{\partial Q_{1+n_0}}{\partial\delta_2} & \cdots & \dfrac{\partial Q_{1+n_0}}{\partial\delta_n}\end{bmatrix} \tag{2.17}$$

$$J_{22}=\begin{bmatrix} |V_2|\frac{\partial Q_2}{\partial|V_2|} & \cdots & |V_{1+n_0}|\frac{\partial Q_2}{\partial|V_{1+n_0}|} \\ \vdots & \ddots & \vdots \\ |V_2|\frac{\partial Q_{1+n_0}}{\partial|V_n|} & \cdots & |V_{1+n_0}|\frac{\partial Q_{1+n_0}}{\partial|V_{1+n_0}|} \end{bmatrix} \tag{2.18}$$

➢ Load Flow Algorithm

The Newton-Raphson procedure is as follows:

Step-1: Choose the initial values of the voltage magnitudes $|V|^{(0)}$ of all n_p load buses and $n-1$ angles $\delta^{(0)}$ of the voltages of all the buses except the slack bus.

Step-2: Use the estimated $|V|^{(0)}$ and $\delta^{(0)}$ to calculate a total $n-1$ number of injected real power $P_{calc}^{(0)}$ and equal number of real power mismatch $\Delta P^{(0)}$.

Step-3: Use the estimated $|V|^{(0)}$ and $\delta^{(0)}$ to calculate a total n_p number of injected reactive power $Q_{calc}^{(0)}$ and equal number of reactive power mismatch $\Delta Q^{(0)}$.

Step-3: Use the estimated $|V|^{(0)}$ and $\delta^{(0)}$ to formulate the Jacobian matrix $J^{(0)}$.

Step-4: Solve (4.30) for $\delta^{(0)}$ and $\Delta|V|^{(0)} \div |V|^{(0)}$

Step-5 : Obtain the updates from

$$\delta^{(1)}=\delta^{(0)}+\Delta\delta^{(0)} \tag{2.19}$$

$$|V|^{(1)}=|V|^{(0)}\left[1+\frac{\Delta|V|^{(0)}}{|V|^{(0)}}\right] \tag{2.20}$$

Step-6: Check if all the mismatches are below a small number. Terminate the process if yes. Otherwise go back to step-1 to start the next iteration with the updates given by (2.19) and (2.20).

2.4.3 Fast Decoupled Method

The fast decoupled power flow method is a very fast and efficient method of obtaining power flow problem solution. In this method, both, the speeds as well as the sparsity are exploited. This is actually an extension of Newton-Raphson method formulated in polar coordinates with certain approximations which result into a fast algorithm for power flow solution.

This method exploits the property of the power system where in MW flow-voltage angle and MVAR flow-voltage magnitude are loosely coupled. In other words a small change in the magnitude of the bus voltage does not affect the real power flow at the bus and similarly a small change in phase angle of the bus voltage has hardly any effect on reactive power flow.

Because of this loose physical interaction between MW and MVAR flows in a power system, the MW- δ and MVAR-V calculations can be decoupled. This decoupling results in a very simple, fast and reliable algorithm. As we know, the sparsity feature of admittance matrix minimizes the computer memory requirements and results in faster computations. The accuracy is comparable to that of the N-R method.

using N-R method can be written in polar coordinates as –

$$\begin{bmatrix} \Delta P \\ \Delta Q \end{bmatrix} = \begin{bmatrix} H & N \\ M & L \end{bmatrix} \begin{bmatrix} \Delta \delta \\ \frac{\Delta V}{V} \end{bmatrix}$$

where H, N, M and L are the elements (viz., $J_{1,}$ J_2, J_3 and J_4) of the Jacobian matrix.

Since changes in real power (i.e., ΔP) are less sensitive to the changes in voltage magnitude (i.e., ΔV) and changes in reactive power (i.e., ΔQ) are less sensitive to the changes in phase angle of voltage (i.e., Δδ), Eq. (6.131) can be reduced to –

$$\begin{bmatrix} \Delta P \\ \Delta Q \end{bmatrix} = \begin{bmatrix} H & 0 \\ 0 & L \end{bmatrix} \begin{bmatrix} \Delta \delta \\ \frac{\Delta V}{V} \end{bmatrix}$$

Expansion of above equation

$$\Delta P = H \Delta \delta$$

$$\Delta Q = L \frac{\Delta V}{V}$$

Off-diagonal element of H is –

$$\begin{aligned} H_{ik} = \tfrac{\partial P_i}{\partial Q_k} &= V_i V_k Y_{ik} \sin(\theta_{ik} + \delta_i - \delta_k) \\ &= V_i V_k Y_{ik} [\sin\theta_{ik} \cos(\delta_i - \delta_k) + \cos\theta_{ik} \sin(\delta_i - \delta_k)] \\ &= V_i V_k [Y_{ik} \sin\theta_{ik} \cos(\delta_i - \delta_k) + Y_{ik} \cos\theta_{ik} \sin(\delta_i - \delta_k)] \\ &= V_i V_k [-B_{ik} \cos(\delta_i - \delta_k) + G_{ik} \sin(\delta_i - \delta_k)] \end{aligned} \tag{2.21}$$

Similarly off-diagonal element of L is –

$$L_{ik} = \frac{\partial Q_i V_k}{\partial V_k} = V_i V_k Y_{ik} \sin(\theta_{ik} + \delta_i - \delta_k)$$

$$= V_i V_k [-B_{ik} \cos(\delta_i - \delta_k) + G_{ik} \sin(\delta_i - \delta_k)] \tag{2.22}$$

From Eq. (2.21) and (2.22) we have

$$H_{ik} = L_{ik} = V_i V_k [-B_{ik} \cos(\delta_i - \delta_k) + G_{ik} \sin(\delta_i - \delta_k)]$$

The diagonal elements of H are given as –

$$H_{ii} = \frac{\partial P_i}{\partial \delta_i} = -\sum_{\substack{k=1 \\ k \neq i}}^{n} V_i V_k Y_{ik} \sin(\theta_{ik} + \delta_i - \delta_k)$$

$$= -Q_i + V_i V_i Y_{ii} \sin \theta_{ii} = -Q_i - {V_i}^2 B_{ii}$$

Similarly diagonal elements for the matrix are given as –

$$L_{ii} = \frac{\partial Q_i V_i}{\partial V_i} = 2{V_i}^2 Y_{ii} \sin \theta_{ii} + \sum_{\substack{k=1 \\ k \neq i}}^{n} V_i V_k Y_{ik} \sin(\theta_{ik} + \delta_i - \delta_k)$$

$$= 2{V_i}^2 Y_{ii} \sin \theta_{ii} + Q_i - {V_i}^2 Y_{ii} \sin \theta_{ii}$$

$$= Q_i + {V_i}^2 Y_{ii} \sin \theta_{ii} = Q_i - {V_i}^2 B_{ii}$$

In the case of fast decoupled power flow method of power flow studies the following approximations are made for evaluating Jacobian elements.

$$\cos(\delta_i - \delta_k) \approx 1$$

$$G_{ik} \sin(\delta_i - \delta_k) \leq B_{ik}$$

$$Q_i \ll {V_i}^2 B_{ii}$$

With the above assumptions the Jacobian elements become –

$$H_{ik} = L_{ik} = -V_i V_k B_{ik} \text{ for } k \neq i$$

$$H_{ii} = L_{ii} = -{V_i}^2 B_{ii}$$

With these Jacobian elements

$$\Delta P_i = H \Delta \delta = V_i V_k B'_{ik} \Delta \delta_k \tag{2.23}$$

and $\Delta Q_i = L \frac{\Delta V}{V} = V_i V_k B'_{ik} \frac{\Delta V_k}{V_k}$ (2.24)

Further decoupling and final algorithm for the fast-decoupled power-flow studies are obtained by:

1. Omitting from B', the representation of those network elements that affect MVAR flows, i.e., shunt reactance and off-nominal in phase transformer taps.

2. Omitting from B", the angle shifting affects of phase shifters.

3. Dividing Eqs. (6.141) and (6.142) by V_i and assuming V_k = 1.0 pu and also neglecting series resistance in calculating the elements of B'.

With the above assumptions, Eqs. (2.23) and (2.24) for the power flow studies become:

$$\frac{\Delta P_i}{V_i} = B'\Delta\delta \tag{2.25}$$

$$\frac{\Delta Q_i}{V_i} = B''\Delta V \tag{2.26}$$

In the above equations B' and B" are real and sparse and have similar structures as those of H and L respectively. Since, they contain only network admittances, they are constant and do not change during successive iterations for solution of power flow problem, they need to be evaluated only once and inverted once during the first iteration and then used in all successive iterations.

It is due to the nature of Jacobian matrices B' and B" and the sparsity of these matrices that the method is fast. In this method of power flow studies, each cycle of iteration consists of one solution for Δδ to update δ and one solution for ΔV to update V. The iterations are continued till ΔP and ΔQ at all load buses and Δ P at all generation buses are within prescribed (or assumed) tolerances.

Chapter 3

Description of GENROU

3.1 Introduction

The round rotor synchronous generator is equipped with stator and rotor, where, its rotor is examined in terms of the mechanical power and speed that ultimately lead to produce voltage on its stator windings. Therefore, the working principle of this generator mainly focuses on its mechanical power, rotor speed, the voltage across its field windings (field voltage) and the voltage across its stator terminals (terminal voltage). The round rotor synchronous generator (GENROU)is an important power equipment in thermal energy, mainly steam turbine.

The study of synchronous generator helps in providing a useful knowledge required in static and dynamic analysis of bulk power systems. The usefulness of this work results in knowing the system status under controlled constraints. The dynamic model of GENROU is developed by a set of algebraic equations that control voltage and current phasors during both normal and abnormal situations. Besides, in the development of generator's dynamic model, the differential equations of rotor speed and the flux linkages are included to control the instantaneous values of voltage and power.

3.2 Mathematical Modeling

3.2.1 Round Rotor Synchronous Generator (GENROU)

Testing of dynamic models of GENROU was performed in Simulink and PSS/e platforms. A number of algebraic equations identical to real time model of GENROU were written in Simulink. Thereafter, the same equations were matched with built-in GENROU models in PSS/e for the precision check.

Therefore, the mathematical models of both direct and quadrature axes of the generator are formulated Simulink for the simulation purpose. The emf voltage across q-axis winding of GENROU (E_q') mainly depends upon the field current due to d-axis (I_{fd}), the d-axis armature reactance (X_{ad}), the field voltage across d-axis winding (E_{fd}) and the d-axis open circuit transient time constant (T_{d0}').

$$\dot{E}_q' = \frac{1}{T_{d0}{}'}(E_{fd} - X_{ad} I_{fd}) \tag{3.1}$$

Similarly, the emf voltage across d-axis winding of GENROU (E'_d) mainly depends upon the field current due to q-axis (I_{fq}), the q-axis armature reactance (X_{aq}), and the q-axis open circuit transient time constant (T'_{q0}), i.e.

$$\dot{E}'_d = \frac{1}{T_{q0}{}'}(-1)(X_{aq}I_q) \tag{3.2}$$

Furthermore, the sub transient flux linkage in d and q-axes (ψ'') of GENROU is produced after induced voltage in both generator windings as shown in Eq. (3.3)

$$\psi''_d = \frac{E'_q(X''_d - X_l) + \psi_{kd}(X'_d - X''_d)}{X'_d - X_l} \tag{3.3}$$

$$\psi''_q = \frac{-E'_d\left(X''_q - X_l\right) + \psi_{kq}(X'_q - X''_q)}{X'_q - X_l}$$

Now, as shown in Eq. (3.4), the resultant flux linkage in the synchronous generator will be the sum of mutual flux-linkages in quadrature and direct axes windings during the sub-transient (initial) period.

$$|\psi''| = \sqrt{(\psi''_d)^2 + \left(\psi''_q\right)^2}$$

$$\psi_d = \psi''_d - X''_d i_d \tag{3.4}$$

$$\psi_q = \psi''_q - X''_q i_q$$

3.2.2 GENROU Model Without Saturation

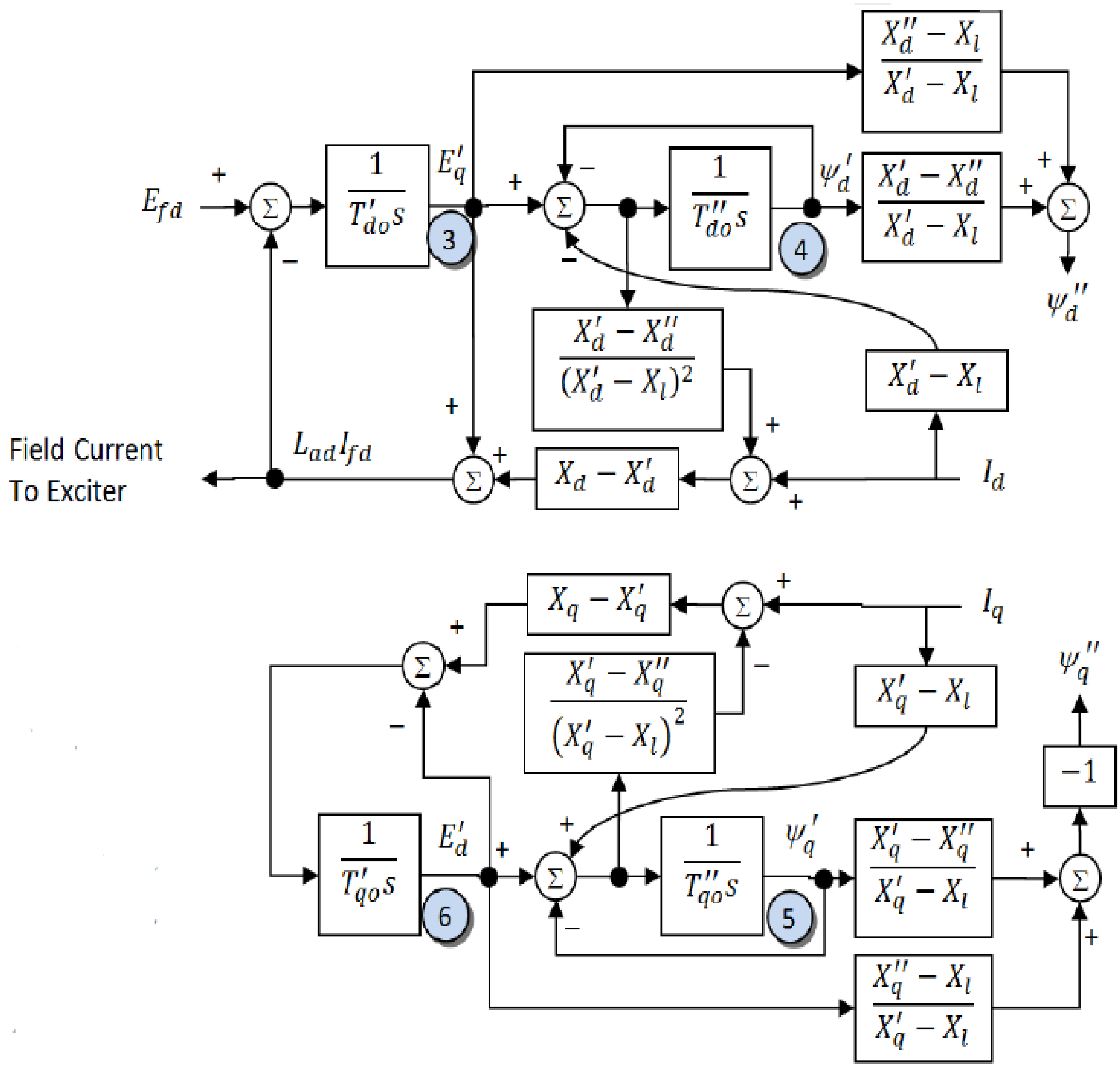

Figure 3.1 : GENROU Model Without Saturation.

3.2.3 GENROU Model With Saturation

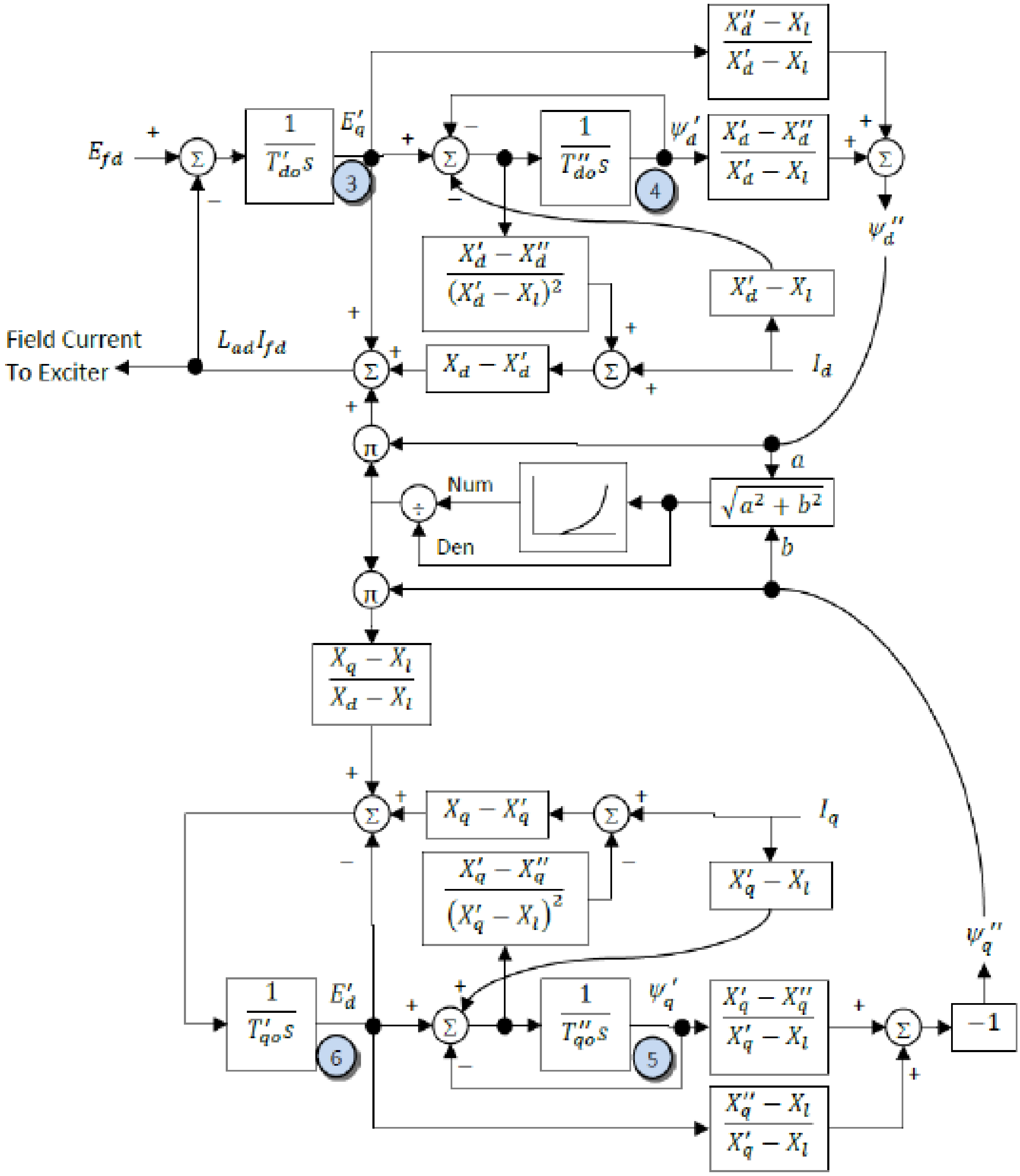

Figure 3.2 : GENROU Model With Saturation.

3.3 GENROU Parameters

Input Data for GENROU

Parameters	Description	Value	Unit
T'_{do}	d-axis open circuit transient time constant	6.5	Second
T''_{do}	d-axis open circuit sub-transient time constant	0.13	Second
T'_{qo}	q-axis open circuit transient time constant	1.25	Second
T''_{qo}	q-axis open circuit sub-transient time constant	0.13	Second
H	inertia	4	MW.s/MVA
D	damping	0	pu
X_d	d-axis synchronous reactance	0.1	pu
X_q	q-axis synchronous reactance	0.11	pu
X'_d	d-axis transient reactance	0.1	pu
X'_q	q-axis transient reactance	0.12	pu
X''_d	d-axis sub-transient reactance	0.02	pu
X''_q	q-axis sub-transient reactance	0.02	pu
X_l	leakage reactance	0.2	pu
S(1.0)	Saturation factor at 1.0 pu	0.03	pu
S(1.2)	Saturation factor at 1.2 pu	0.03	pu
Ra	Armature resistance	0	pu
X_p	Potier reactance	0.185	pu

Table 3.1 : Input parameters of GENROU

Default Parameters for GENROU

Parameters	Description	Value	Unit
T'_{do}	d-axis open circuit transient time constant	9.697	Second
T''_{do}	d-axis open circuit sub-transient time constant	0.048	Second
T'_{qo}	q-axis open circuit transient time constant	1.164	Second
T''_{qo}	q-axis open circuit sub-transient time constant	0.087	Second
H	inertia	6.29	MW.s/MVA
D	damping	0	pu
X_d	d-axis synchronous reactance	1.685	pu
X_q	q-axis synchronous reactance	1.641	pu
X'_d	d-axis transient reactance	0.214	pu
X'_q	q-axis transient reactance	0.388	pu
X''_d	d-axis sub-transient reactance	0.16	pu
X''_q	q-axis sub-transient reactance	0.16	pu
X_l	leakage reactance	0.137	pu
S(1.0)	Saturation factor at 1.0 pu	0.114	pu
S(1.2)	Saturation factor at 1.2 pu	0.489	pu
Ra	Armature resistance	0.0006	pu
X_p	Potier reactancce	0.182	pu

Table 3.2 : Default parameters of GENROU

Chapter 4

Wind Turbine Generator Model

4.1 Introduction

Modern wind power plants (WPPs), comprised of a large number of wind turbine generators (WTGs), a collector system, collector and/or interconnect substation utilize machines that are designed to optimize the generation of power using the energy in the wind. WTGs have developed from small machines with output power ratings on the order of kilowatts to several megawatts, and from machines with limited speed control and other capabilities to machines with variable speed control capabilities over a wide speed range and sophisticated control capabilities using modern power electronics.

The application of WTGs in modern WPPs requires an understanding of a number of different aspects related to the design and capabilities of the machines involved. This paper, authored by members of the Wind Plant Collector Design Working Group of the IEEE, is intended to provide insight into the various wind turbine generator designs, based on classification by machine type and speed control capabilities, along with their operational characteristics, voltage, reactive power, or power factor control capabilities, voltage ride-through characteristics, behavior during short circuits, and reactive power capabilities.

4.2 Turbine Characteristics

4.2.1 Type 1 Wind Turbine Generator

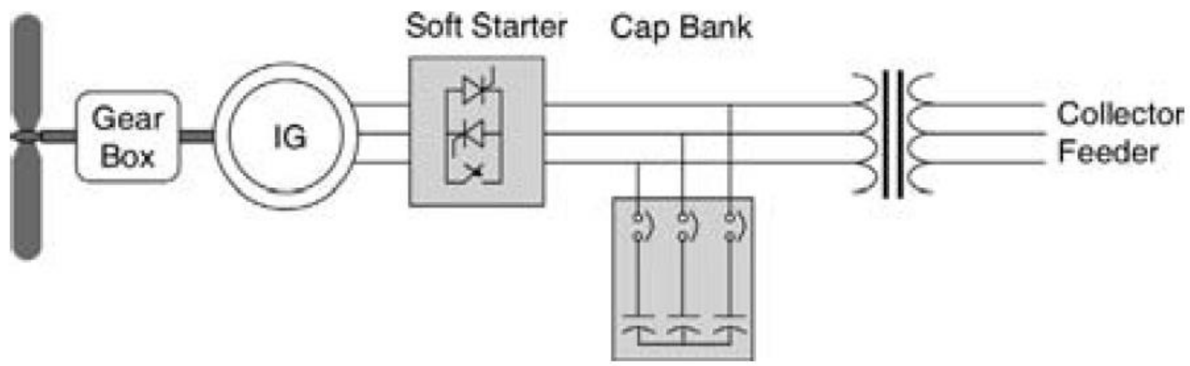

Figure 4.1 : Type 1 Wind Turbine Generator (WT1G)

The Type 1 WTG is implemented with a squirrel-cage induction generator (SCIG) and is connected to the step up transformer directly. See Figure 1.

The turbine speed is fixed (or nearly fixed) to the electrical grid's frequency, and generates real power (P) when the turbine shaft rotates faster than the electrical grid frequency creating a negative slip (positive slip and power is motoring convention).

Figure 4.1 shows the power flow at the SCIG terminals. While there is a bit of variability in output with the slip of the machine, Type 1 turbines typically operate at or very close to a rated speed. A major drawback of the induction machine is the reactive power that it consumes for its excitation field and the large currents the machine can draw when started ''across-the-line.'' To ameliorate these effects the turbine typically employs a soft starter and discrete steps of capacitor banks within the turbine.

4.2.2 Type 2 Wind Turbine Generator

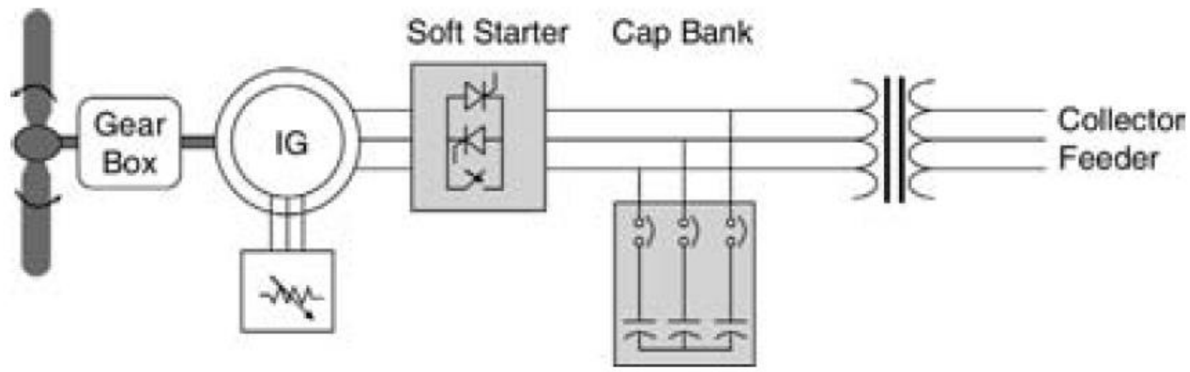

Figure 4.2 : Type 2 Wind Turbine Generator (WT2G)

In Type 2 turbines, wound rotor induction generators arc connected directly to the WTG step-up transformer in a fashion similar to Type 1 with regards to the machines stator circuit, but also include a variable resistor in the rotor circuit. See Figure 3. This can be accomplished with a set of resistors and power electronics external to the rotor with currents flowing between the resistors and rotor via slip rings. Alternately, the resistors and electronics can be mounted on the rotor, eliminating the slip rings—this is the Wrier design. The variable resistors are connected into the rotor circuit softly and can control the rotor currents quite rapidly so as to keep constant power even during gusting conditions, and can influence the machine's dynamic response during grid disturbances.

As stated earlier, Type 1 and Type 2 WTGs typically use PFCCs to maintain the power factor or reactive power of the machine to a specified setpoint. The PFCCs may be sized to maintain a slightly leading (inductive) power factor of around 0.98 at rated power output. This is often referred to as no-load compensation. With full-load compensation, the PFCCs are sized to maintain unity power factor or, in some cases, a slightly lagging (capacitive) power factor at the machine's rated power output. The PFCCs typically consists of multiple stages of capacitors switched with a low-voltage AC contactor.

4.2.3 Type 3 Wind Turbine Generator

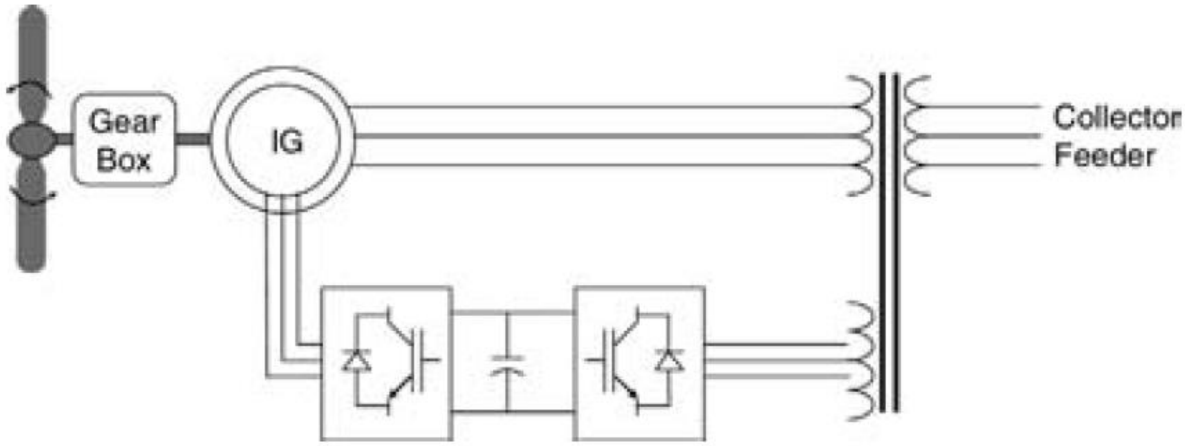

Figure 4.3 : Type 3 Wind Turbine Generator (WT3G)

The Type 3 turbine, known commonly as the Doubly Fed Induction Generator (DFIG) or Doubly Fed Asynchronous Generator (DFAG), takes the Type 2 design to the next level, by adding variable frequency ac excitation (instead of simply resistance) to the rotor circuit. The additional rotor excitation is supplied via slip rings by a current regulated, voltage-source converter, which can adjust the rotor currents' magnitude and phase nearly instantaneously. This rotor-side converter is connected back-to-back with a grid side converter, which exchanges power directly with the grid. See Figure 4.3.

A small amount power injected into the rotor circuit can effect a large control of power in the stator circuit. This is a major advantage of the DFIG—a great deal of control of the output is available with the presence of a set of converters that typically are only 30% of the rating of the machine. In addition to the real power that is delivered to the grid from the generator's stator circuit, power is delivered to the grid through the grid-connected inverter when the generator is moving faster than synchronous speed. When the generator is moving slower than synchronous speed, real power flows from the grid, through both converters, and from rotor to stator. These two modes, made possible by the four-quadrant nature of the two converters, allows a much wider speed range, both above and below synchronous speed by up to 50%, although narrower ranges are more common.

The greatest advantage of the DFIG, is that it offers the benefits of separate real and reactive power control, much like a traditional synchronous generator, while being able to run asynchronously. The field of industrial drives has produced and matured the concepts of vector or field oriented control of induction machines. Using these control schemes, the torque producing components of the rotor flux can be made to respond fast enough that the machine remains under relative control, even during significant grid disturbances. Indeed, while more expensive than the Type 1 or 2 machines, the Type 3 is becoming popular due to its advantages.

Type 3 (DFIG) WTGs typically have a reactive power capability corresponding to a power factor of 0.95 lagging (capacitive) to 0.90 leading (inductive) at the terminals of the machines. Options for these machines include an expanded reactive power capability of 0.90 lagging to 0.90 leading. Some Type 3 WTGs can deliver reactive power even when the turbine is not operating mechanically, while no real power is generated.

The model is based on the detailed General Electric (GE) wind turbine model and consists of four components: generator/converter, converter control, wind turbine, and pitch control. Several simplifications were made to the General Electric Wind Turbine Generator (WTG) model, for instance: the active power control and General Electric Wind Inertia control were excluded. In the generic Type 3 generator/converter model, the flux dynamics are eliminated to reflect the rapid response of the converter to the higher level commands from the electrical controls.

The model also includes a Low Voltage Power Logic (which can be bypassed) used to limit the real current command during and immediately following sustained faults. The converter control model consists of two components: the reactive and active power control modules. The converter control dictates the active and reactive power to be delivered to the system via the current and voltage commands to the generator, E_{pcmd}, and E_{qcmd}, respectively. The reactive power order, Q_{ord}, can either be held constant or be computed by a separate model, the Wind Plant Reactive Power Control Emulator or the power factor regulator.

The Wind Plant Reactive Power Control Emulation represents a simplified equivalent of the supervisory V_{Ar} controller portion of the entire wind farm management system. The active power order is derived from the generator power and speed. The speed reference, ref, is obtained from a turbine speed set point vs. power output f(Pgen) curve. A very simplified aerodynamic model is used in the Type 3 generic WTG model. This model does not require the representation of the power coefficient curve. In the pitch controller model, the blade position actuators are rate-limited and there is a time constant associated with the translation of blade angle to mechanical output. The pitch control consists of two PI controllers that act on the speed and power errors.

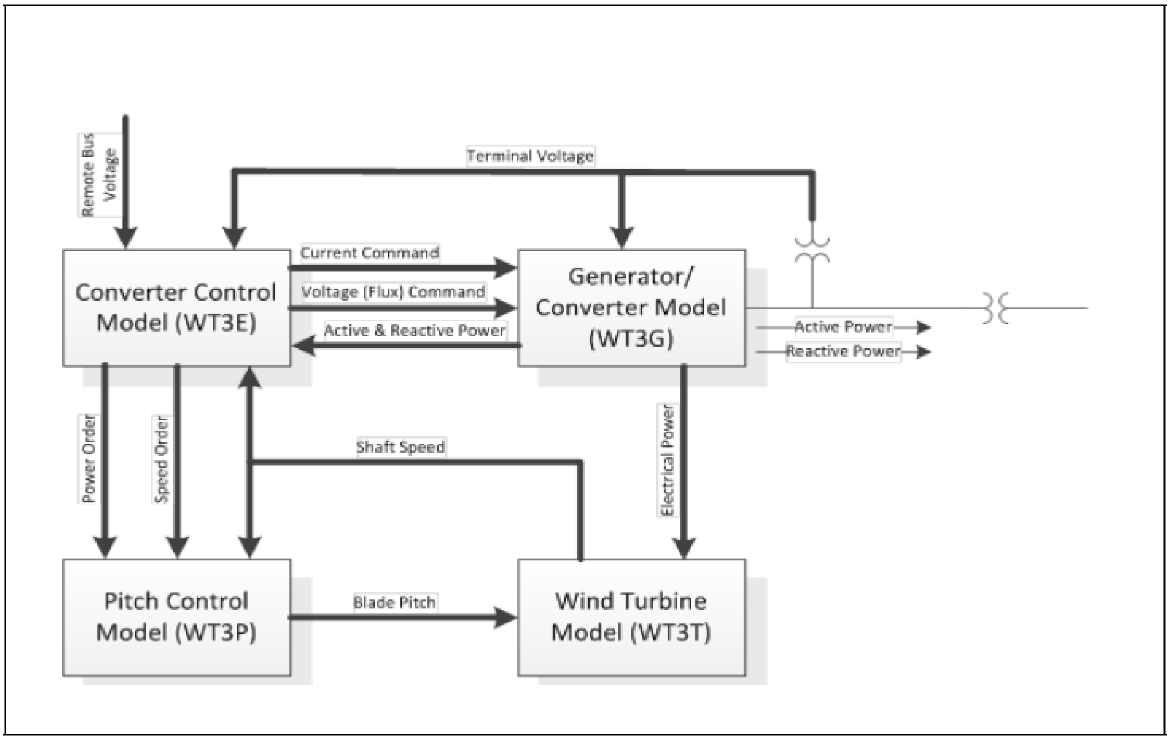

Figure 4.4 : WT3 modeling package

The WT3 modeling package includes 4 main models as follows:

1.Generator/Converter Model WT3G
2.Electrical control model (converter control) for the Generic Wind Model WT3E
3.Mechanical control (wind turbine) for the WT3 Generic Wind Model WT3T
4.Pitch control model for the WT3 Generic Wind Model WT3P

WIND PLANT SPECIFIC ADJUSTMENTS:

- V_{arflag} and V_{ltflag} are flags that must be set by the user based on the setting defined for each WPP to be included in the case study.

- F_n = Fraction of WTG on the wind plant that are on-line. Used only for VAR control gain adjustment PFA_{ref} = initialized from load ow data.

- V_c is the controlled bus specified within the module WT3E. It can be terminal voltage or remote bus voltage or fictitious remote bus voltage.

- X_c is a fictitious reactance used to compute the voltage drop to offset the reference voltage of a known bus voltage V_{rfq} and a known branch current I_{reg}.

$$(V_c = \left|V_{rfq}.jX_c.I_{reg}\right|)$$

- V_w >1.0 p.u. will be used to initialize pitch angle.

4.3 Generator/Converter Model (WT3G)

This model (WT3G) is an equivalent of the generator and the field converter and provides the interface between the WTG and the network. Unlike a conventional generator model, it contains no mechanical state variables for the machine rotor {these are included in the turbine model (WT3T). Further, unlike conventional generator models, all of the flux dynamics have been eliminated to reflect the rapid response to the higher level commands from the electrical controls through the converter. The net result is an algebraic, controlled-current source that computes the required injected current into the network in response to the flux and active current commands from the electrical control model. For modeling an aggregation of several (N) WTGs, MVAb must equal the N times the MVA rating of a single WTG. There are two different generator/converter models available, namely WT3G1 and WT3G2. The WT3G2 model, which is recommended for new dynamic setups, includes improvements in the original WT3G1. The original WT3G1 model is being retained for reasons of backward compatibility.

Input data for WT3 Generator

Constants	Description	Default Value
J	(Tiqcmd, Converter time constant for IQcmd)	0.20
J+1	(Tipcmd, Converter time constant for IPcmd)	0.0
J+2	(KPLL, PLL gain)	0.0
J+3	(KIPLL, PLL integrator gain)	0.0
J+4	(PLLMAX, PLL max. limit)	0.10
J+5	(Prated)	1.50
J+6	(VLVPL1, LVPL voltage 1 Low voltage power logic)	0.50
J+7	(VLVPL2, LVPL voltage 2)	0.90
J+8	(GLVPL, LVPL gain)	1.0
J+9	(VHVRCR, High Voltage Reactive Current (HVRC) logic, pu voltage)	1.20
J+10	(CURHVRCR, HVRC logic, current (pu))	2.0
J+11	(RIp LVPL, Rate of active current change)	5.0
J+12	(T LVPL, Voltage sensor for LVPL, second)	0.02
STATES	**Description**	
K	Converter lag for Ipcmd	
K+1	Converter lag for Eqcmd	
K+2	PLL FIrst integrator	
K+3	PLL second integrator	
K+4	Voltage sensor for LVPL	
VARs	**Description**	
L	(delta Q), over voltage correction factor	
ICONs	**Description**	
M	Number of lumped wind turbines	

Table 4.1 : Input data for WT3 Generator Model

Block Diagram of WT3 Generator

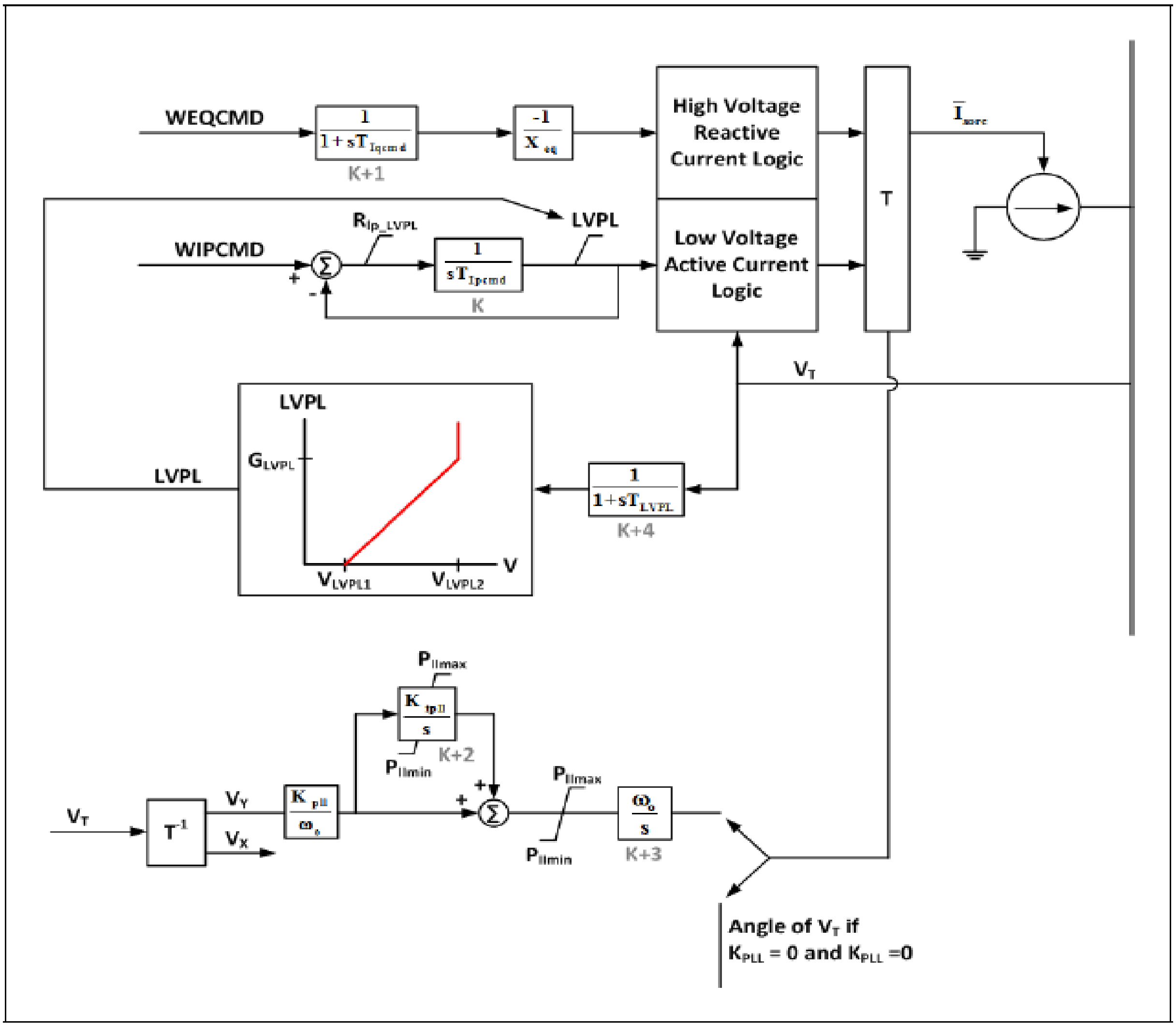

Figure 4.5 : Block Diagram of WT3 Generator Model

High-voltage reactive current management and Low-voltage active current management represent logic associated with the dynamic model and the ac network solution. The actual implementation of this logic may be software dependent.

4.3.1 Turbine Model (WT3T)

The turbine WT3T model uses the two-mass representation of the wind turbine shaft drive train. It calculates the speed deviations of the rotor on the machine and the blade sides. By setting the turbine inertia fraction Htfrac = 0 the model can be switched to a conventional single mass representation.

Input data for WT3 Turbine

Constants	Description	Default Value
J	(VW, Initial wind, pu of rated wind speed)	1.25
J+1	(H, Total inertia constant, sec)	4.95
J+2	(DAMP, Machine damping factor, pu P/pu speed)	0.0
J+3	(Kaero, Aerodynamic gain factor)	0.7e-02
J+4	(Theta2, Blade pitch at twice rated wind speed, deg.)	21.98
J+5	(Htfrac, Turbine inertia fraction (Hturb/H)[1])	0.0
J+6	(Freq1, First shaft torsional resonant frequency, Hz)	1.8
J+7	(Dshaft, Shaft damping factor (pu))	1.5
K	(Shaft twist angle, rad.)	
K+1	(Shaft twist angle, rad.)	
K+2	(Generator speed deviation, pu)	
K+3	(Generator rotor angle deviation, pu)	
VARs	**Description**	
L	Paero on the rotor blade side, pu	
L+1	Initial rotor slip	
L+2	Initial internal angle	
L+3	Initial pitch angle	
L+4	Paero initial	

Table 4.2 : Input data for WT3 Turbine Model

Block Diagram (Dual Mass)

To simulate one-mass mechanical system, set Htfrac -0. To simulate two-mass mechanical system, set Htfrac as 0 <Htfrac <1

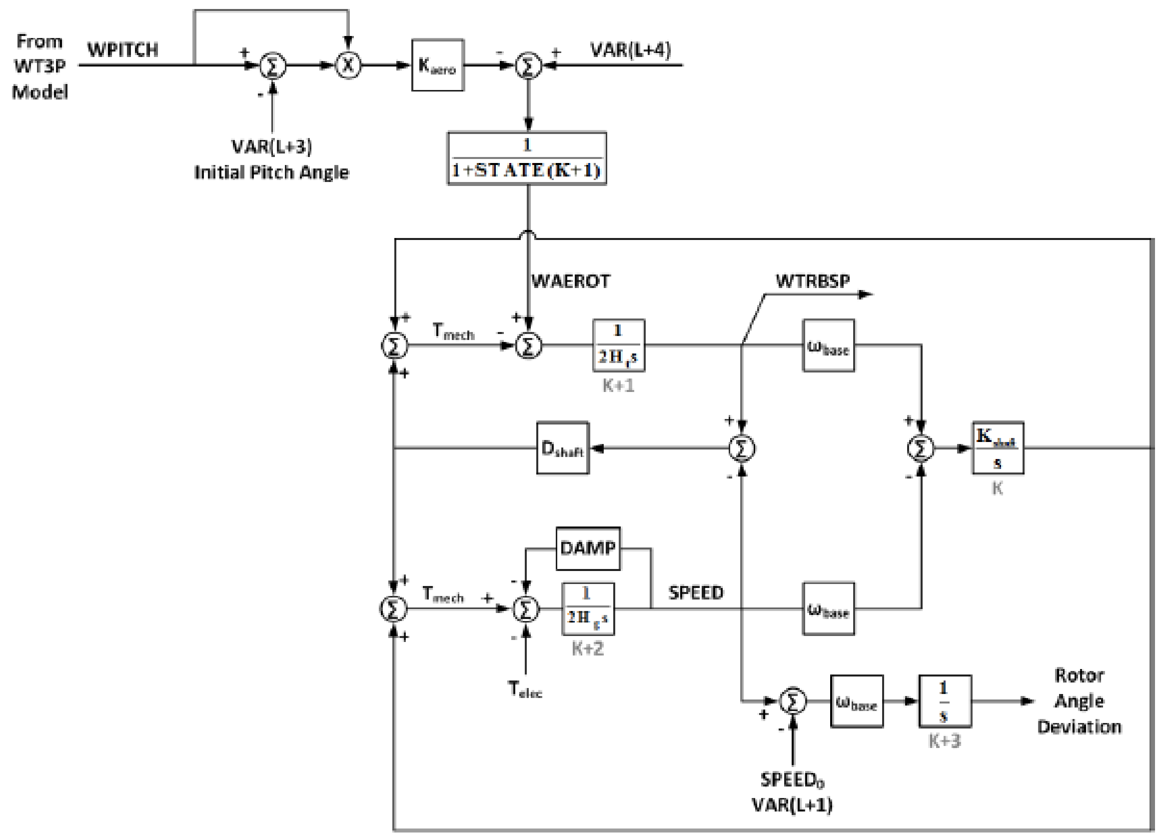

$H_t = H_{tfrac} \times H$

$H_g = H - H_t$

$$K_{shaft} = \frac{2H_t \times H_g \times (2\pi \times Freq1)^2}{H \times \omega_0}$$

Figure 4.6 : Block Diagram of WT3 Turbine Model

4.3.2 Pitch Control Model (WT3P)

Pitch control is the technology used to operate and control the angle of the blades in a wind turbine. The system is in general either made up of electric motors and gears or hydraulic cylinders and a power supply system. The pitch system is a closed-loop drive system. The turbine main controller calculates the required pitch angle from a set of conditions, such as wind speed, generator speed, and power production. The required pitch angle is transferred to the pitch system as a set point. If the actual angle is NOT the same as the set point, the system will direct power to the electric motor or fluid to the cylinder to make the actuator move the blade to the required angle.

Input data for WT3 Pitch Control

Constants	Description	Default Value
J	(Tp, Blade response time constant)	0.30
J+1	(Kpp, Proportional gain of PI regulator (pu))	150.0
J+2	(Kip, Integrator gain of PI regulator (pu))	25.0
J+3	3.0(Kpc, Proportional gain of the compensator (pu))	3.0
J+4	(Kic, Integrator gain of the compensator (pu))	30.0
J+5	(TetaMin, Lower pitch angle limit (degrees))	0.0
J+6	(TetaMax, Upper pitch angle limit (degrees))	27.0
J+7	(RTetaMax, Upper pitch angle rate limit (degrees/sec))	10.0
J+8	(PMX, Power reference, pu on MBASE)	1.0
K	(Shaft twist angle, rad.)	
K+1	(Turbine rotor speed deviation, pu)	
K+2	(Generator speed deviation, pu)	
K+3	(Generator rotor angle deviation, pu)	
STATEs	**Description**	
K	Output lag	
K+1	Pitch control	
K+2	Pitch compensation	

Table 4.3: Input data for WT3 Pitch Control Model

Block Diagram of WT3 Pitch Control Model

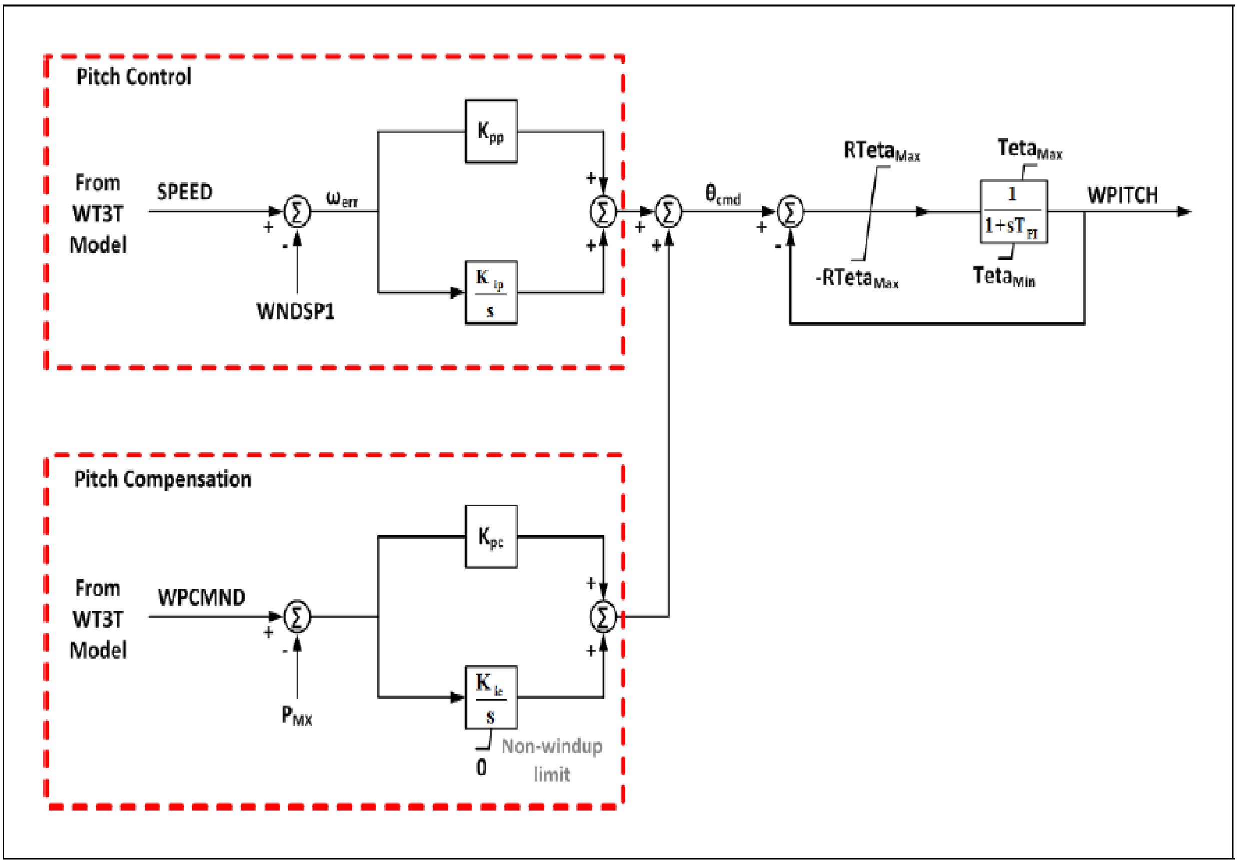

Figure 4.7 : Block Diagram of WT3 Pitch Control Model

4.3.3 Converter Control Model (WT3E)

This model (WT3E) dictates the active and reactive power to be delivered to the system. The reactive controls including the emulation of the centralized Wind Plant reactive power controller are shown below. The switch, VARFLG, provides for 3 modes of control: constant reactive power, constant power factor angle, or voltage regulation by a wind plant reactive power controller. The switch, VLTFLG, provides for bypassing the closed- loop terminal voltage regulator, which is not used in all implementations and currently always set to 1. The non-linear function, f(Pelech), is used to model the desired WTG speed as a function of the power level. The input data for this function are values of the desired speed at several levels of power output, with linear interpolation to be used between specified values. The electrical control model WT3E can be used with WT3G1as well as with the improved WT3G2 models. When WT3E is used with the WT3G1model, it is recommended that ICON(M+2) be set to 1, and when used with WT3G2, the ICON(M+2) be set to 2. Input data for WT3E.

Input data for Converter Control Model (WT3E)

Constants	Description	Default Value
J	Tfv, Filter time constant in voltage regulator (sec)	0.15
J+1	Kpv, Proportional gain in voltage regulator (pu)	18.0
J+2	Kiv, Integrator gain in voltage regulator (pu)	5.0
J+3	Xc, Line drop compensation reactance (pu)	0.0
J+4	TFP, Filter time constant in torque regulator	0.05
J+5	Kpp, Proportional gain in torque regulator (pu)	3.0
J+6	KIP, Integrator gain in torque regulator (pu)	0.6
J+7	PMX, Max limit in torque regulator (pu)	1.12
J+8	PMN, Min limit in torque regulator (pu)	0.1
J+9	QMX, Max limit in voltage regulator (pu)	0.296
J+10	QMN, Min limit in voltage regulator (pu)	-0.436
J+11	IPMAX, Max active current limit	1.10
J+12	TRV, Voltage sensor time constant	0.05
J+13	RPMX, Max power order derivative	0.45
J+14	RPMN, Min power order derivative	-0.45
J+15	T Power, Power filter time constant	5.0
J+16	Kqi, MVAR/Voltage gain	0.05
J+17	VMINCL, Min voltage limit	0.9
J+18	VMAXCL, Max voltage limit	1.2
J+19	Kqv, Voltage/MVAR gain	40.0
J+20	XIQmin	-0.5
J+21	XIQmax	0.4
J+22	Tv, Lag time constant in Wind Var controller	0.05

J+23	Tp, Pelec _lter in fast PF controller	0.05
J+24	Fn, A portion of online wind turbines	1.0
J+25	Pmin, Shaft speed at Pmin (pu)	0.69
J+26	ωP20, Shaft speed at 20% rated power (pu)	0.78
J+27	ωP40, Shaft speed at 40% rated power (pu)	0.98
J+28	ωP60, Shaft speed at 60% rated power (pu))	1.12
J+29	ωPmin, Minimum power for% operating at P100 speed (pu)	0.74
J+30	ωP100, Shaft speed at 100% rated power (pu)	1.20
STATEs	**Description**	
K	Filter in voltage regulator	
K+1	Integrator in voltage regulator	
K+2	Filter in torque regulator	
K+3	Integrator in torque regulator	
K+4	Voltage sensor	
K+5	Power FIlter	
K+6	MVAR/Vref integrator	
K+7	Verror/internal machine voltage integrator	
K+8	Lag of the WindVar controller	
K+9	Input FIlter of Pelec for PF fast controller	
VARs	**Description**	
L	Remote bus ref voltage	
L+1	Q reference if PFAFLG = VARFLG	
L+2	MVAR order from MVAR emulator=0	
L+3	PF angle reference if PFAFLG=1	
L+4	Storage of MW for computation of compensated voltage	
L+5	Storage of MVAR for computation of compensated voltage	
L+6	Storage of MVA for computation of compensated voltage	

ICONs	Description	
M	Remote bus # for voltage control; 0 for local voltage control	
M+1	VARFLG: -1. Constant power factor control 0.	
	Constant Q control 1. Use Wind Plant reactive power control	
M+2	VLTFLG: 0. Bypass terminal voltage control	
	1. Eqcmd limits are calculated as VTerm + XIQmin and VTerm + XIQmax,	
	i.e., limits are functions of terminal voltage	
	2. Eqcmd limits are equal to XIQmin and XIQ max	
M+3	From bus of the interconnection transformer	
M+4	To bus of the interconnection transformer	
M+5	Interconnection transformer ID	

Table 4.4 : Input data for Converter Control Model (WT3E)

Block Diagram of Converter Control Model (WT3E)

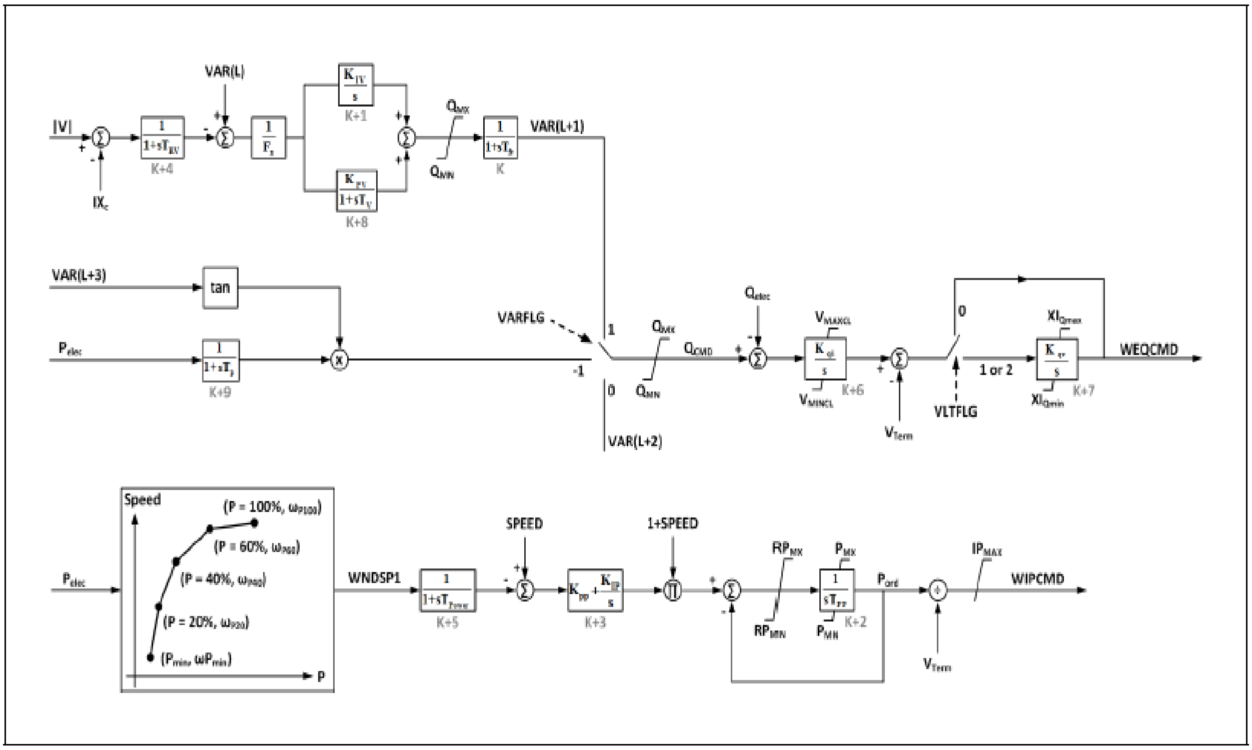

Figure 4.8 : Block Diagram of Converter Control Model (WT3E)

Chapter 5

Grid-Connected Photovoltaic Model

5.1 Introduction

Implementation of the Photo-Voltaic system is costly because of the higher cost solar cells. Efficiency of the system should be improved to get maximum utilization of resources and more algorithms have been developed in this field. Even though the solar energy is available in infinite amount, problem arises in making it physically available for human use. Major method to generate energy from sun is using photovoltaic system (PV system).

Grid connected PV system supply solar electricity through an inverter directly to the household and to the electricity grid if the system is providing more energy than the house needs. The output from the solar panel should be Solar panel delivers the maximum energy at maximum power point. This point of operation should be tracked throughout the period of operation of the PV system.

The grid-connected PV power system can offer a high voltage gain and guarantee the used PV array voltage is less than 50 V, while the power system interfaces the utility grid. he proposed system can not only be applied to the string or multi string inverter system, but also to the module-integrated inverter system in low power applications. On the other hand, the non-isolation PV systems employing neutral-point-clamped topology, highly efficient reliable inverter concept topology, H5 topology, etc., have been widely used especially in Europe. Although the transformer less system having a floating and no earth-connected PV dc bus requires more protection, it has several advantages such as high efficiency, lightweight, etc.

Generated power from the PV module should be converted to a form suitable to be given to the utility grid. The PV module generates a DC voltage. Whereas the grid voltage is 50 Hz AC. From this, it is evident that the PV output should not be connected directly to the utility grid. It should be first boosted to grid voltage level, and then converted to AC which is exactly synchronized to the grid voltage. All these processes need very efficient and accurate control. The control module implemented with a dsPIC30f.It generate PWM signal which controls the operation of the converter and inverter. The digital controller also takes care of the MPPT and synchronization.

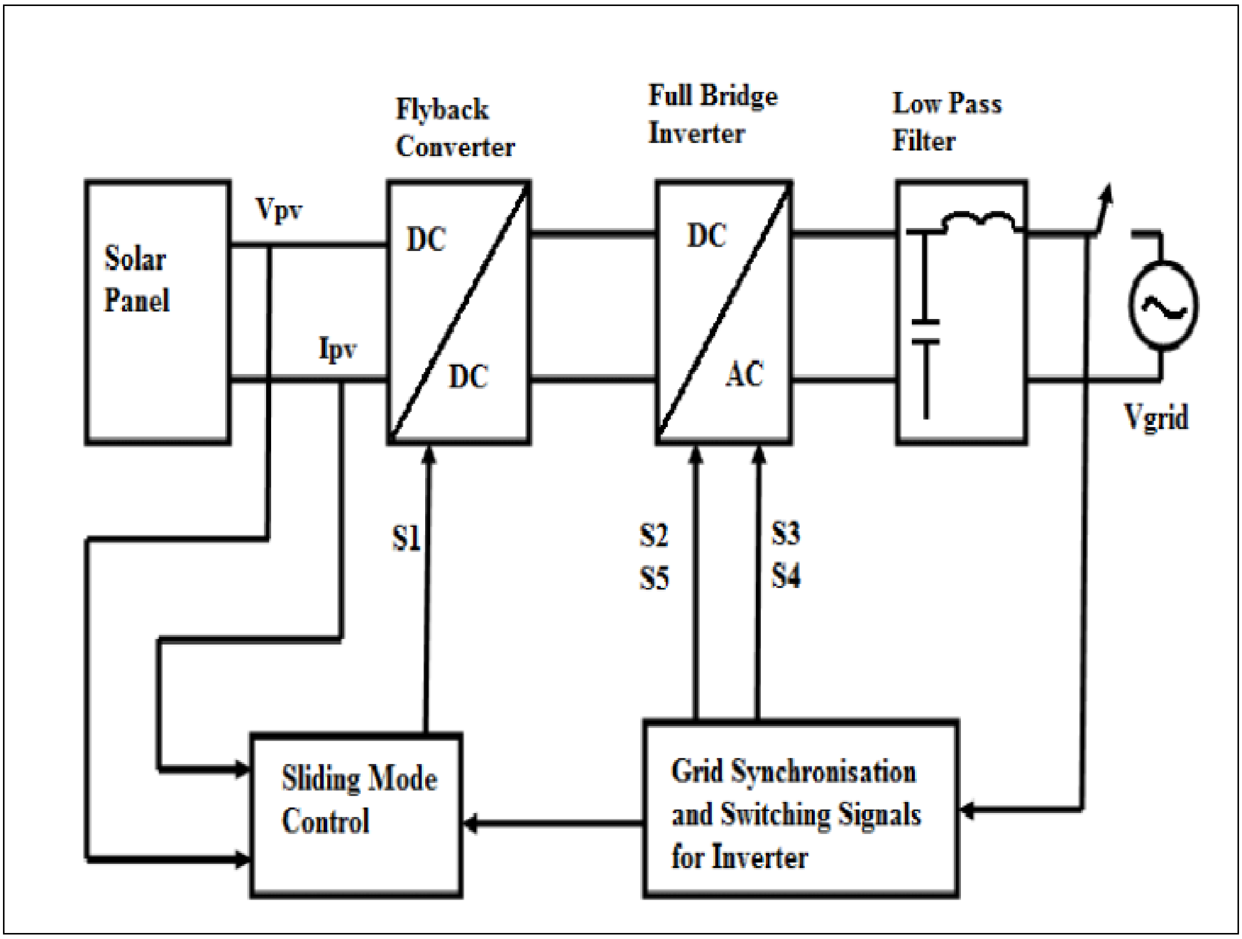

Figure 5.1 : Block diagram of the proposed grid-connected PV inverter system

5.2 Control Module For Grid-Connected PV

A grid-connected photovoltaic (PV) power system is proposed, and the steady-state model analysis and the control strategy of the system are presented. A full-bridge inverter is used as the second power-processing stage, which can stabilize the dc-bus voltage and shape the output current. Interfacing a solar micro inverter module with the power grid involves two major tasks. One is to ensure that the solar micro inverter module is operated at the Maximum Power Point (MPP). The second is to inject a sinusoidal current into the grid. These inverters must be able to detect an islanding situation, and take appropriate action in order to prevent bodily harm and damage to equipment connected to the grid. Two compensation units are added to perform in the system control loops to achieve the low total harmonic distortion and fast dynamic response of the output current. Furthermore, a simple maximum-power-point-tracking method based on power balance is applied in the PV system to reduce the system complexity and cost with a high performance.

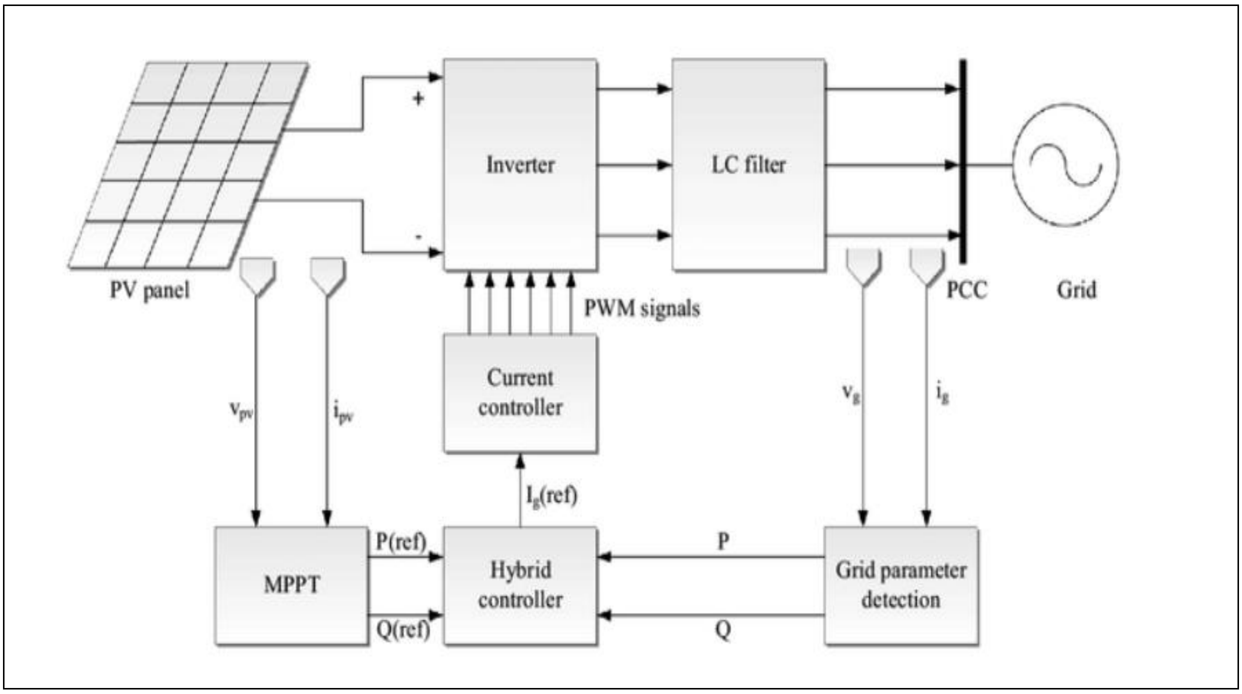

Figure 5.2 **:** Block diagram of the grid connected PV system with controller.

5.3 Operating Temperature and Efficiency of PV Module

Solar irradiance intensity (G) and cell operating temperature (T) are the two crucial parameters which nonlinearly affect the current-voltage as well as power-voltage characteristics of a PV module. In order to model the electrical characteristics of the PV module and its power output, first it is required to determine the cell operating temperature (T) of the PV module.

Standard heat transfer mechanics must be considered to calculate the energy balance on the cell module leading to the prediction of cell temperature. At steady-state conditions, only convection and radiation mechanisms are usually considered, since they are prevalent on the conduction mechanism that merely transports heat toward the surfaces of the mounting frame (especially in the case of rack-mounting free-standing arrays). A survey of the explicit and implicit correlations proposed in literature linking cell temperature with standard weather variables and material and system-dependent properties.

When a resistive load is connected to a PV module, the operating point of the module (which is current and voltage output) is decided by intersection of the I–V characteristics curve of the PV module (which is modeled in Section 3) and the I–V characteristics of the load curve (which is determined from the famous simple electrical correlation, i.e., V=IR). According to the electrical correlation (i.e., V=IR), the slope of the load curve (which is straight line) is expressed as 1/R on I-V plane. The operating point will depend on the value of R (see Figure 5 for visual understanding).

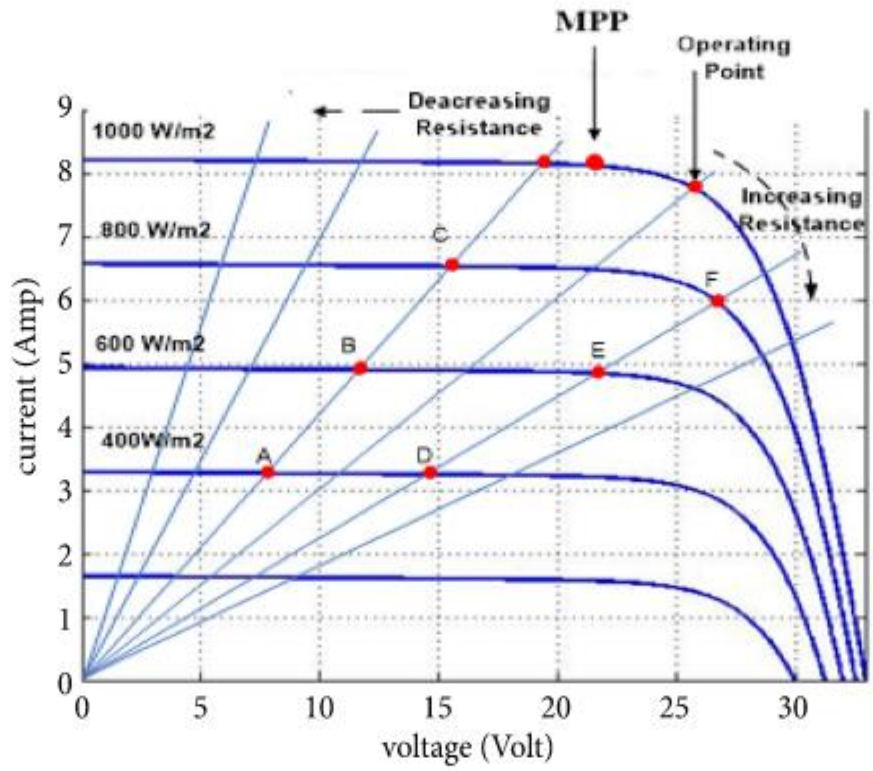

Figure 5.3 : Effect of resistive load on cell operating point.

5.4 Control Module

The Grid-Connected Solar Micro inverter Reference Design is controlled by a single dsPIC DSC device, as shown in the system block diagram. The functions of the dsPIC DSC can be broadly classified into the following categories:

- All power conversion algorithms
- Inverter state machine for the different modes of operation
- Maximum Power Point Tracking (MPPT)
- Digital Phase-Locked Loop (PLL)
- System islanding and Fault handling

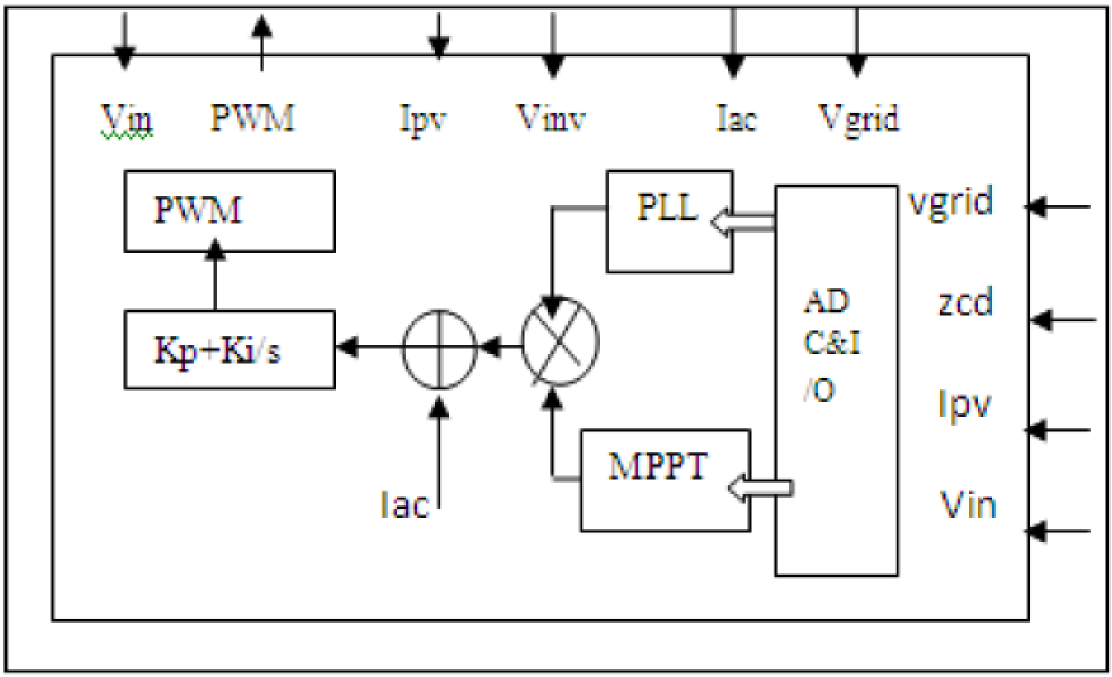

Figure 5.4 : Control module of the grid connected PV system.

The dsPIC DSC device offers intelligent power peripherals specifically designed for power conversion features that applications. These intelligent power peripherals include the High-Speed PWM, High-Speed 10-bit ADC, and High-Speed Analog Comparator modules. These peripheral modules include ease the control of any Switch Mode Power Supply with a high-resolution PWM, flexible ADC triggering, and comparator Fault handling. dsPIC DSC also provides built-in peripherals for digital communications including I2C, SPI and UART modules that can be used for power management and housekeeping functions.

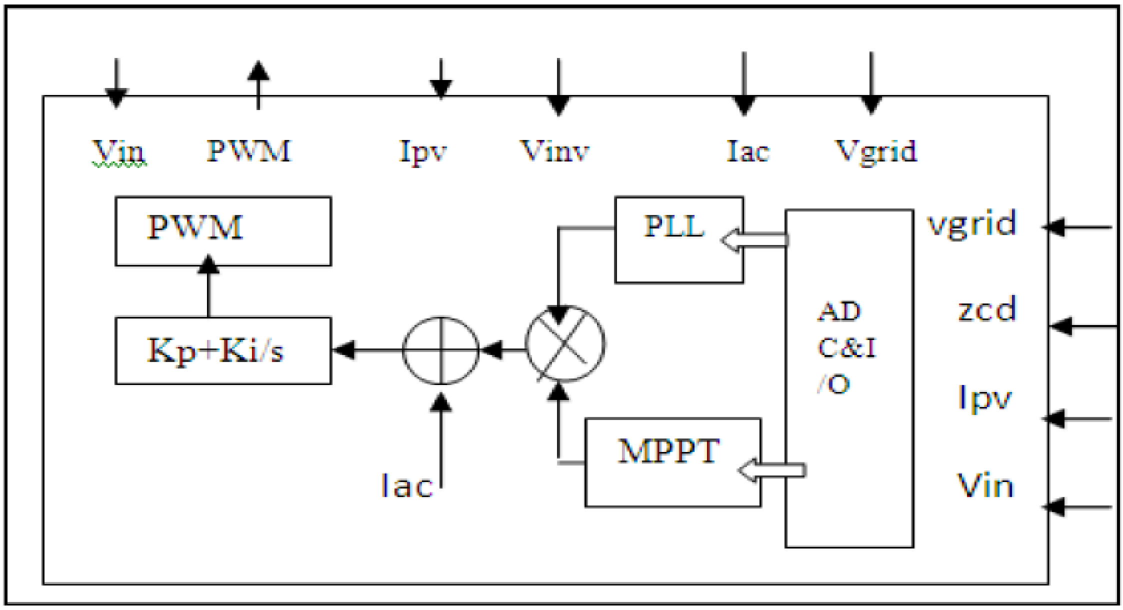

Figure 5.5 : Control loop block diagram.

Chapter 6

Modeling of 37-Bus System

6.1 Model Description

This **37 Bus** Test Case is taken from the text book 'Power System Analysis and Design' by J. Duncan Glover and Mulukutla S. Sarma · It is constructed with three different voltage levels (69 kV, 138 kV and 345 kV), and all units entered in this modeling, are in per unit.This system consists 7 generator,1 pv and 1 wind turbine generator type 3. In this system 43 transmission lines are used which connects the buses. there are 14 transformers used for step up/down for different voltage levels of 69KV,138KV and 345KV.

- Transmission Line Data

From Bus	To Bus	Resistance (R) (pu)	Reactance (X) (pu)	Susceptance (B) (pu)
1	2	0.000750	0.010920	0.117000
1	3	0.001700	0.017000	0.182000
1	6	0.002240	0.032680	0.350000
4	5	0.010280	0.072530	0.017600
4	7	0.011610	0.080850	0.022500
4	13	0.007750	0.052440	0.015400
5	24	0.012430	0.078470	0.019200
7	17	0.004800	0.036800	0.018200
8	11	0.021720	0.069350	0.001900
8	18	0.014200	0.075570	0.069500
8	20	0.027470	0.089090	0.001900
9	12	0.033750	0.078900	0.001200
9	10	0.040500	0.095300	0.002100
10	11	0.027030	0.036130	0.002000
12	16	0.022160	0.090400	0.001700
13	23	0.002040	0.006920	0.160100
14	26	0.014730	0.036000	0.074400
14	27	0.021330	0.052100	0.000900
14	15	0.018240	0.042360	0.007500
14	15	0.018290	0.042460	0.007800
16	26	0.062460	0.082460	0.000300
17	34	0.009020	0.057100	0.013500
18	19	0.003660	0.013120	0.046000
19	21	0.007530	0.005820	0.020600

20	22	0.010170	0.005590	0.025300
20	22	0.010170	0.005590	0.025300
20	25	0.031330	0.076750	0.001500
21	26	0.008460	0.004650	0.021000
21	26	0.008550	0.004700	0.021300
21	26	0.008590	0.004720	0.021400
21	29	0.018350	0.028450	0.022100
24	36	0.007100	0.054400	0.013800
25	28	0.034630	0.082530	0.001600
27	31	0.024230	0.058620	0.001100
27	32	0.042400	0.075090	0.000800
28	29	0.039930	0.099650	0.002000
28	30	0.042110	0.085450	0.047400
30	31	0.026250	0.064290	0.001200
33	32	0.050200	0.101000	0.002500
34	35	0.007350	0.043950	0.012300
34	36	0.018680	0.125900	0.035600
35	37	0.002250	0.013400	0.004000
36	37	0.010300	0.056810	0.016400

Table 6.1 : Transmission Line Data

➢ Transformer Data

From Bus	To Bus	Resistance (R) (pu)	Reactance (X) (pu)	Tap ratio (k)
1	5	0.000870	0.051000	1.00000
2	4	0.000940	0.051070	1.00000
2	4	0.000940	0.051070	1.00000
3	7	0.001000	0.062300	1.00000
4	9	0.001060	0.039490	1.01250
7	8	0.001070	0.040390	1.02500
7	8	0.001070	0.040390	1.02500
13	14	0.001010	0.039250	1.05000
34	28	0.002500	0.071440	1.02125
34	28	0.002440	0.068290	1.02125
6	36	0.000870	0.051000	1.00000
6	36	0.000870	0.051000	1.00000
37	33	0.002500	0.072300	1.00000
23	26	0.001340	0.049880	1.00000

Table 6.2 : Transformer Data

6.2 Load Flow Solution Data of 37-Bus System

A power flow calculation to determine the power flows on transmission lines and transformers and the voltage profile of system bus bars. This calculation is fundamentally important for the planning and design of the connection of wind farms to the transmission grid. N-1 Security criterion is essential for the proper design of transmission networks to ensure the security and reliability of power supply. System performance is compared to operating limits and criteria. Short Circuit calculations also play a very significant role in the proper selection of high voltage equipment and the setting of protection relays.

Bus No	V_0 (pu)	angle_0	P_G_0 (MW)	Q_G_0 (MVAr)	P_L_0 (MW)	Q_L_0 (MVAr)
1	1.030000	0.000000	147.2283	2.081500	0.000000	0.000000
2	1.027161	-0.785502	0.000000	0.000000	0.000000	0.000000
3	1.027842	-0.894705	0.000000	0.000000	0.000000	0.000000
4	1.021427	-2.648033	0.000000	0.000000	0.000000	0.000000
5	1.028211	-1.023194	0.000000	0.000000	0.000000	0.000000
6	1.030000	2.160415	300.0000	-27.53020	0.000000	0.000000
7	1.021233	-4.205389	0.000000	0.000000	0.000000	0.000000
8	0.993686	-5.574021	0.000000	0.000000	23.00000	7.000000
9	1.002805	-4.473004	0.000000	0.000000	17.00000	3.000000
10	0.984360	-6.016455	0.000000	0.000000	18.00000	5.000000
11	0.980619	-6.265757	0.000000	0.000000	33.00000	13.00000
12	0.989910	-5.984925	0.000000	0.000000	23.00000	7.000000
13	1.010161	-4.304253	0.000000	0.000000	0.000000	0.000000
14	1.020000	-6.884270	16.00000	237.4547	56.00000	13.00000
15	1.007690	-7.625506	0.000000	0.000000	74.00000	27.00000
16	0.992639	-6.623547	0.000000	0.000000	23.00000	6.000000
17	1.023414	-4.515342	0.000000	0.000000	12.00000	5.000000
18	0.996717	-6.466170	0.000000	0.000000	20.00000	6.000000
19	0.997806	-6.475108	0.000000	0.000000	58.00000	4.000000
20	0.979674	-8.429020	0.000000	0.000000	45.00000	12.00000
21	1.004869	-6.470963	0.000000	0.000000	58.00000	36.00000
22	0.978253	-8.472377	0.000000	0.000000	27.00000	3.000000
23	1.000000	-3.918056	140.0000	-189.9300	0.000000	0.000000
24	1.028542	-0.828206	0.000000	0.000000	14.00000	4.000000
25	0.995400	-7.830231	0.000000	0.000000	14.00000	3.000000
26	1.010000	-6.458667	75.00000	69.02210	0.000000	0.000000
27	1.012401	-6.783375	0.000000	0.000000	15.00000	5.000000
28	1.020000	-6.622171	20.00000	84.55460	60.00000	12.00000
29	1.001724	-6.928450	0.000000	0.000000	36.00000	10.00000
30	1.010000	-7.292160	10.00000	11.02870	22.00000	15.00000
31	1.007459	-7.401999	0.000000	0.000000	23.00000	3.000000
32	1.020000	-5.259445	38.00000	-1.676100	1400000	3.000000
33	1.021229	-4.713446	0.000000	0.000000	28.00000	6.000000
34	1.029526	-4.642993	0.000080	0.000000	0.000000	0.000000
35	1.024760	-3.720880	0.000000	0.000000	23.00000	6.000000
36	1.030912	-0.290719	0.000000	0.000000	0.000000	0.000000
37	1.024558	-3.276425	0.000000	0.000000	0.000000	0.000000

Table 6.3 : Load Flow Solution for 37-Bus System

6.3 Power Flow Modeling Data

6.3.1 Generator Data

GENROU Data (genrou 1 and genrou 2)

Symbol	**Description**	**Value**	**Unit**
V_b	Base Voltage of Bus	345	KV
V_0	Voltage Magnitude	1.03	pu
angle_0	Voltage angle	2.160415	deg.
P_0	Active power	150	MW
Q_0	Reactive power	-13.7651	MVAr
M_b	Machine base power	160	MVA

Table 6.4 : Generator 1 (genrou 1) and Generator 2 (genrou 2) Power Flow Data

GENROU Data (genrou 3)

Symbol	**Description**	**Value**	**Unit**
V_b	Base Voltage of Bus	69	KV
V_0	Voltage Magnitude	1.02	pu
angle_0	Voltage angle	-5.259445	deg.
P_0	Active power	38	MW
Q_0	Reactive power	-1.6761	MVAr
M_b	Machine base power	50	MVA

Table 6.5 : Generator 3 (genrou 3) Power Flow Data

GENROU Data (genrou 4)

Symbol	Description	Value	Unit
V_b	Base Voltage of Bus	69	KV
V_0	Voltage Magnitude	1.02	pu
angle_0	Voltage angle	-6.622171	deg.
P_0	Active power	20	MW
Q_0	Reactive power	84.5546	MVAr
M_b	Machine base power	100	MVA

Table 6.6 : Generator 4 (genrou 4) Power Flow Data

GENROU Data (genrou 5)

Symbol	Description	Value	Unit
V_b	Base Voltage of Bus	69	KV
V_0	Voltage Magnitude	1.02	pu
angle_0	Voltage angle	-6.884270	deg.
P_0	Active power	16	MW
Q_0	Reactive power	237.4547	MVAr
M_b	Machine base power	250	MVA

Table 6.7 : Generator 5 (genrou 5) Power Flow Data

GENROU Data (genrou 6)

Symbol	Description	Value	Unit
V_b	Base Voltage of Bus	138	KV
V_0	Voltage Magnitude	1.0	pu
angle_0	Voltage angle	-3.918056	deg.
P_0	Active power	140	MW
Q_0	Reactive power	-189.9300	MVAr
M_b	Machine base power	250	MVA

Table 6.8 : Generator 6 (genrou 6) Power Flow Data

GENROU Data (genrou 7)

Symbol	Description	Value	Unit
V_b	Base Voltage of Bus	345	KV
V_0	Voltage Magnitude	1.0	pu
angle_0	Voltage angle	0	deg.
P_0	Active power	147.2283	MW
Q_0	Reactive power	2.0815	MVAr
M_b	Machine base power	160	MVA

Table 6.9 : Generator 7 (genrou 7) Power Flow Data

6.3.2 Photovoltaic Data

Symbol	Description	Value	Unit
S_b	System Base Power	100	MVA
V_0	Voltage Magnitude	1.01	pu
angle_0	Voltage angle	-7.292160	deg.
P_0	Active power	10	MW
Q_0	Reactive power	11.0287	MVAr
Sn	Nominal Power	160	MVA
Vref	Voltage Reference	1.0002	pu
Td	d-axis Inverter Time Constant	0.15	Second
Tq	q-axis Inverter Time Constant	0.15	Second
Ki	Integral gain of the voltage controller	50.9005	
Kp	Proportional gain of the voltage controller	0.0868	

Table 6.10 : PV Power Flow Data and Parameters

6.3.3 Wind Turbine Generator Data

Wind Generator (wt3g) Data

Symbol	Description	Value	Unit
V_b	Base Voltage of the Bus	69	KV
V_0	Voltage Magnitude	1.01	pu
angle_0	Voltage angle	-6.458667	deg.
P_0	Active power	75	MW
Q_0	Reactive power	69.0221	MVAr
M_b	Machine Base power	100	MVA
X_eq	Equivalent reactance for current injection	0.8	pu
K_pll	PLL first integrator gain	20	
K_ipll	PLL second integrator gain	0.6	
Pll_max	PLL max limit	0.5	
P_rated	Turbine rating	1	

Table 6.11 : Wind generator (wt3g) Power Flow Data and Parameters

6.4 Implementation in OpenModelica Using OpenIPSL

6.4.1 Case-1 (Modeling with GENROU)

In this case GENROU connected at all generator buses. Renewable energy resources are not used in this case. This case is only for verifying the result when 37 bus system connected with GENROU.

Model 6.1

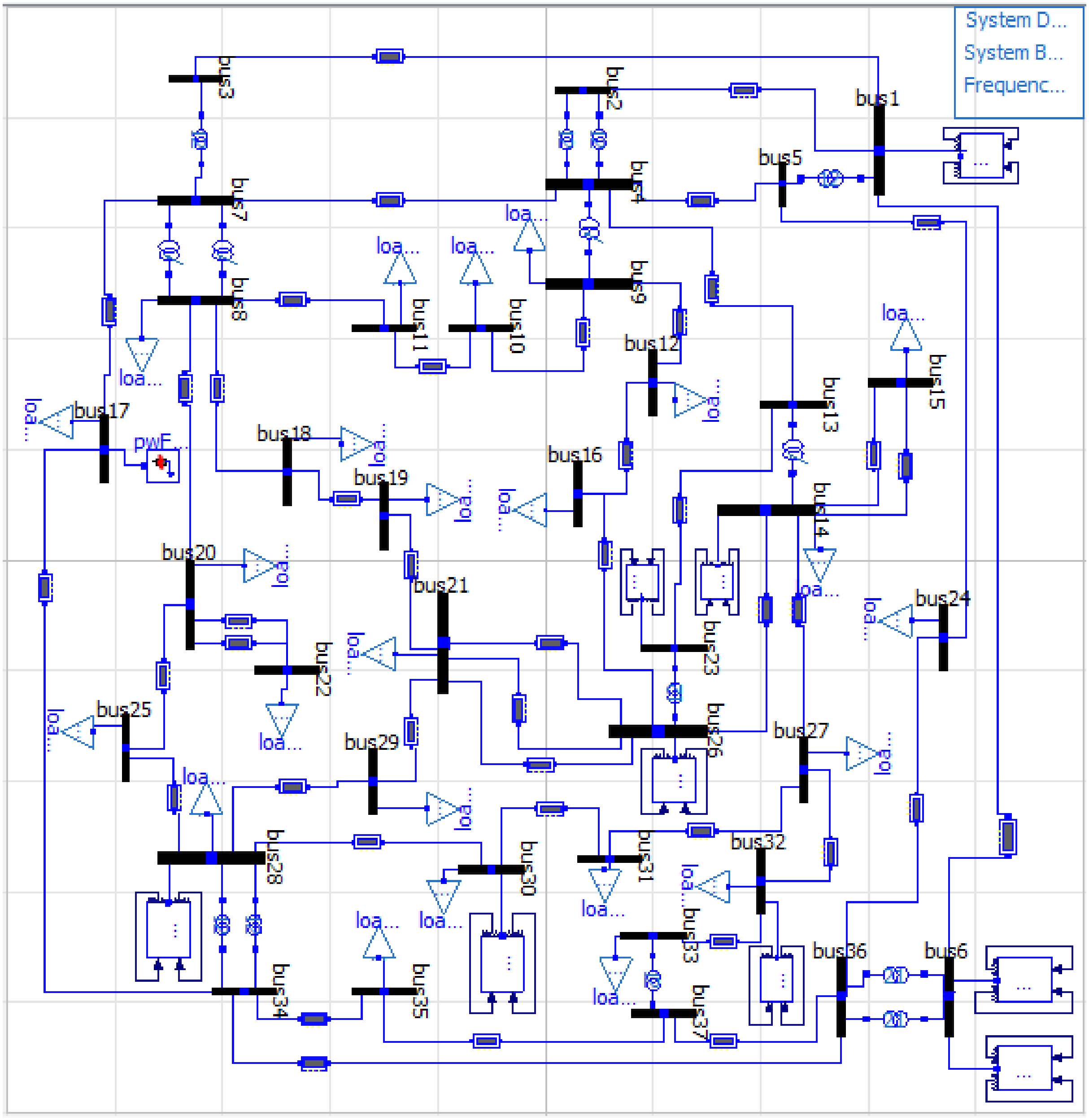

Figure 6.1 : Connection of Glover 37-Bus System Using OpenIPSL

6.4.2 Case-2 (Modeling with GENROU and PV)

In this model both GENROU and PV are connected at generator bus. This is renewable energy integration by using solar system. Slack bus connected with generator but bus no 30 generator replaced with constant PV model. This modeling is only for checking response of buses voltage when system connected with solar.

Model 6.2

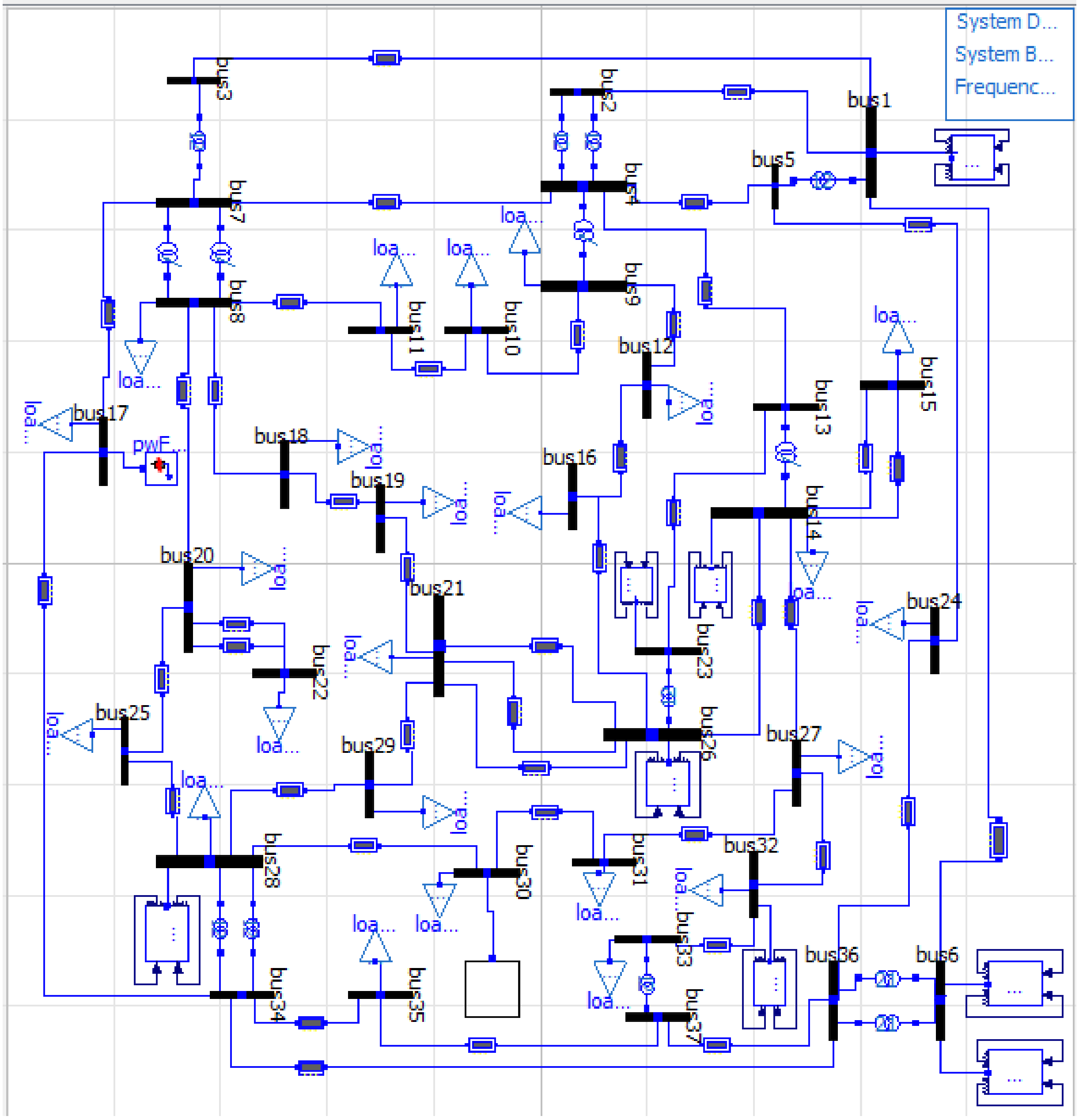

Figure 6.2 : Solar Connected 37 Bus System Using OpenIPSL

6.4.3 Case 3 (Modeling With GENROU, PV and WT3G)

Model 6.3

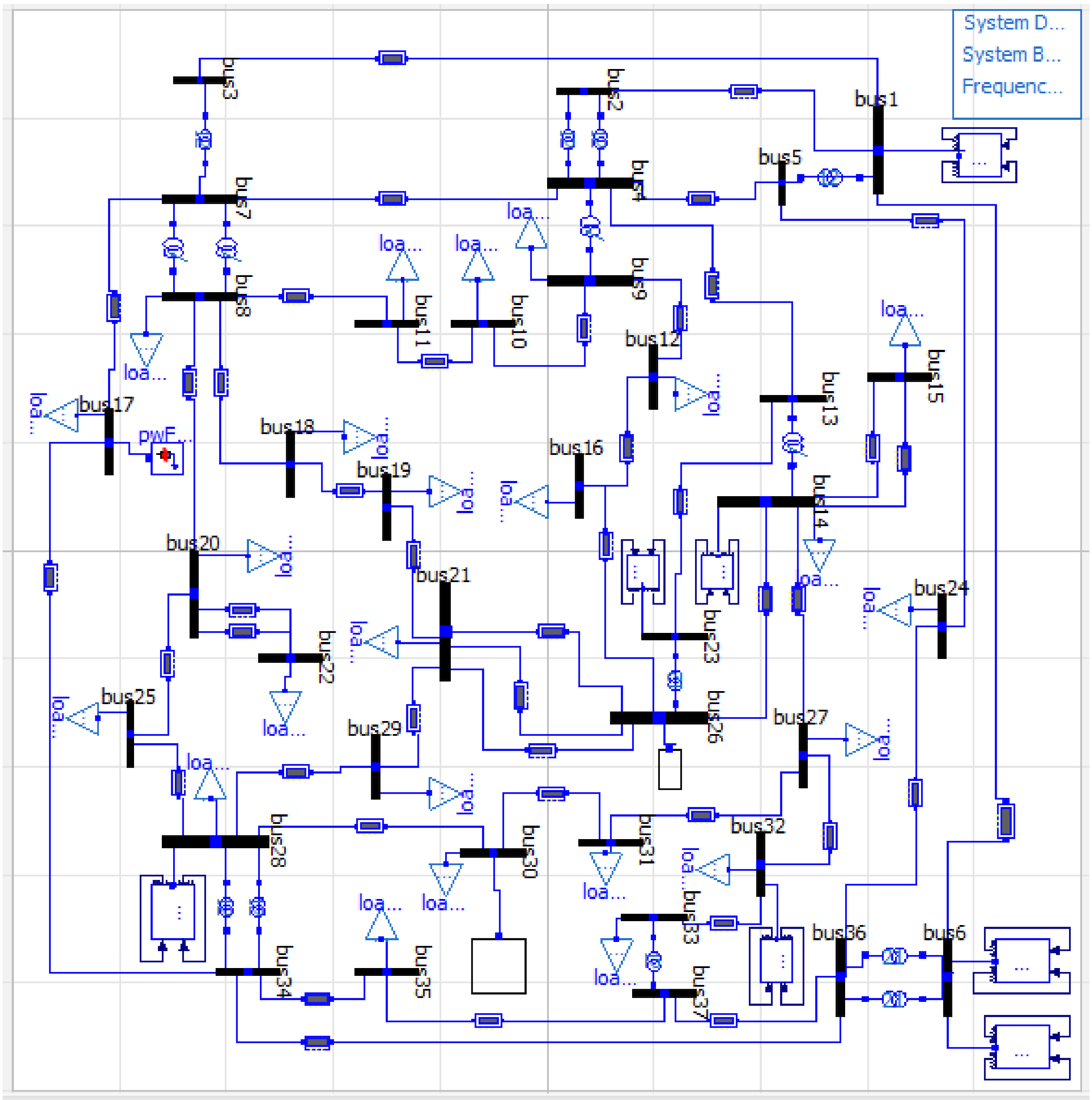

Figure 6.3 : Glover 37-Bus System Integrated with PV and WT3G Using OpenIPSL

37 bus system is modeled for renewable energy integration. A GENROU (genrou 7) is connected with slack bus (bus no 1) which operates at 345KV, (genrou 1) and (genrou 2) is connected with bus no 6 at 345KV, (genrou 3) is connected with bus no 32 at 69KV, (genrou 4) is connected with bus no 28 at 69KV, (genrou 5) is connected with bus no 14 at 69KV and (genrou 6) is connected with bus no 23 at 138KV. For renewable energy a constant PV is connected with bus no 30 at 69 KV and a wind turbine generator has connected with bus no 26 at 69 KV.

Chapter 7

Simulation Result

For all simulations, the following conditions were applied:

- The fault applied is a bolted symmetrical three-phase applied one second after the start of the simulation.
- The fault clearing time is 0.6 second and the simulation time is 10 seconds.

7.1 Case-1

This case is the simulation result of Model 6.1 (page 49).

7.1.1 Buses Voltage Response

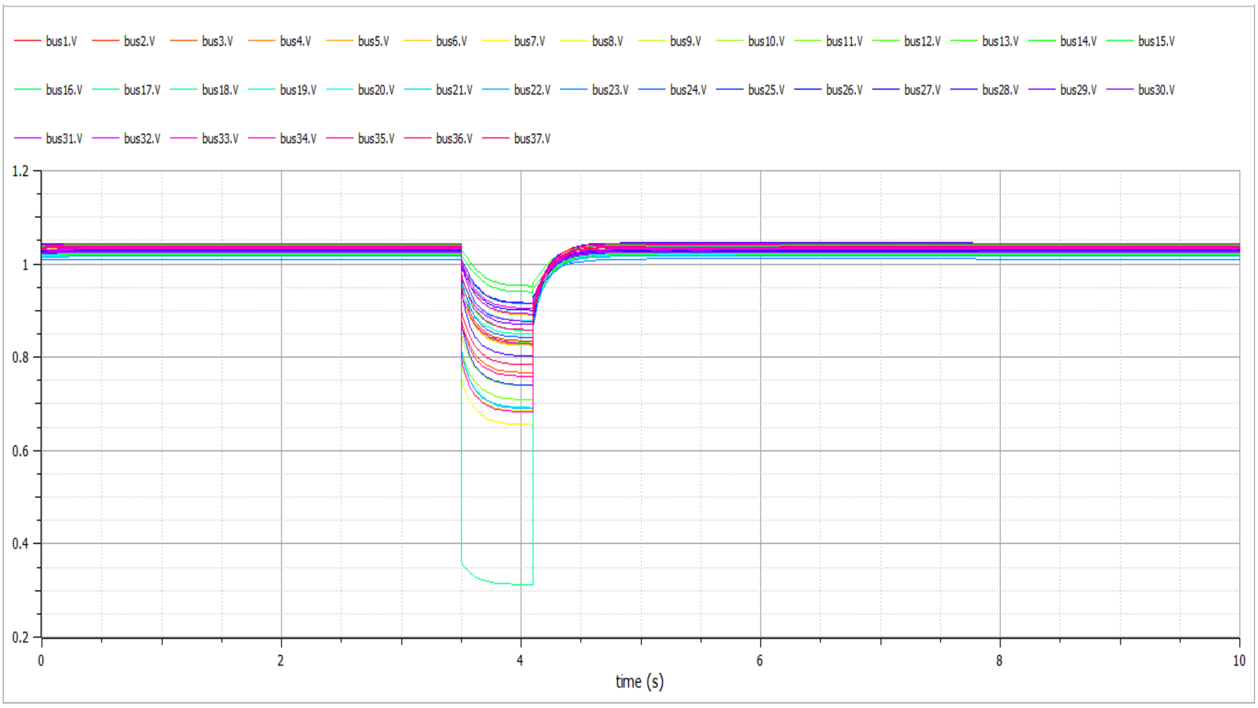

Figure 7.1 : All 37 buses voltage Profile Under Fault

Figure 7.1 shows that when simulation reached at 3.5 second suddenly buses voltage dips due to fault and when fault is cleared after 4.1 second voltage recovers after some oscillation.

7.1.2 Active Power Response of Generators

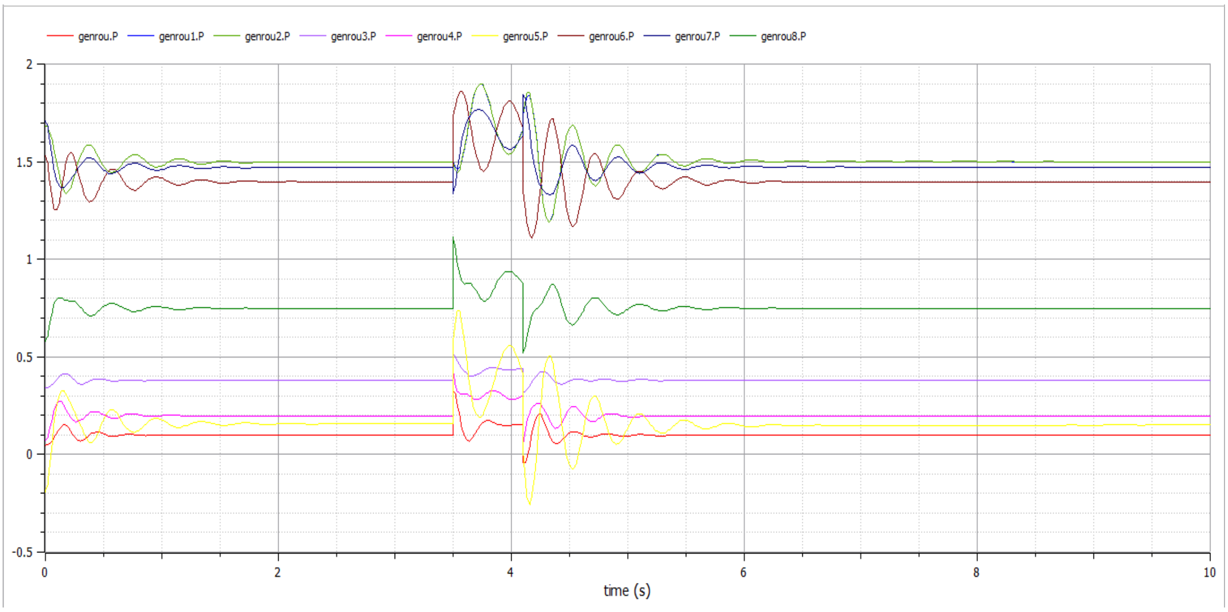

Figure 7.2 : Active Power Response of Generators Under Fault

7.1.3 Reactive Power Response of Generators

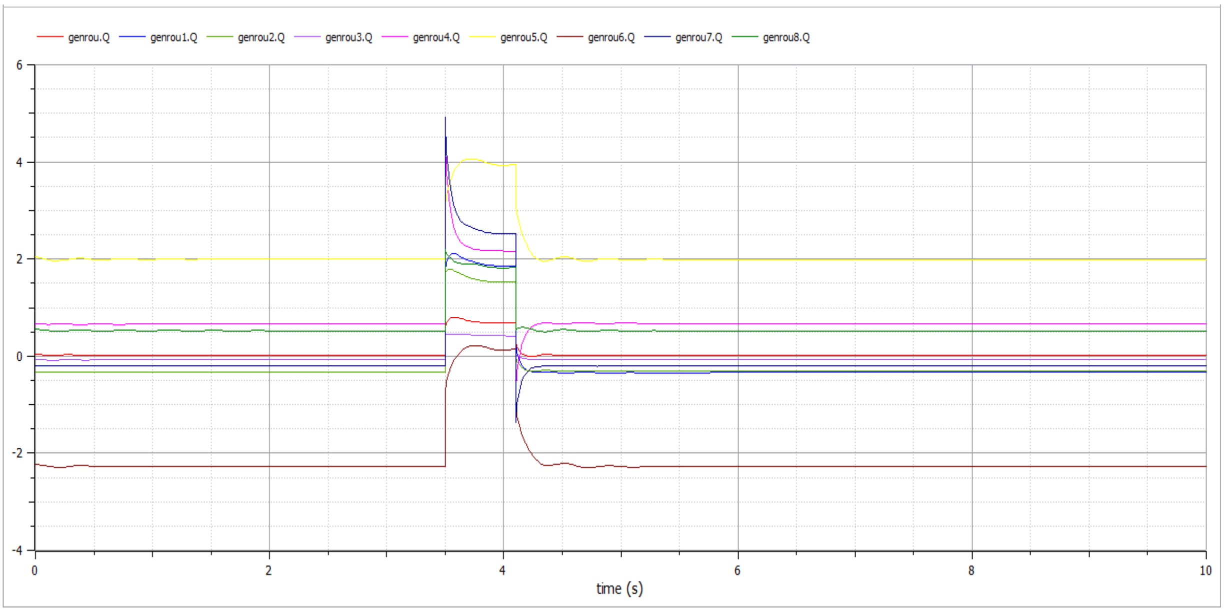

Figure 7.3 : Reactive Power Response of Generators Under Fault

In Figure 7.2 we can see when simulation reached at fault time large fluctuation occurred in active power and when fault is cleared after some time it become constant. Initial oscillation in plotting of active power is due to staring the generators.

Figure 7.3 Shows the reactive power response after fault. At the time of fault generator provides bulk amount of reactive power to grid for maintain stability.

7.2 Case-2

This case is the simulation result of Model 6.2 (page 50).

7.2.1 Buses Voltage Response

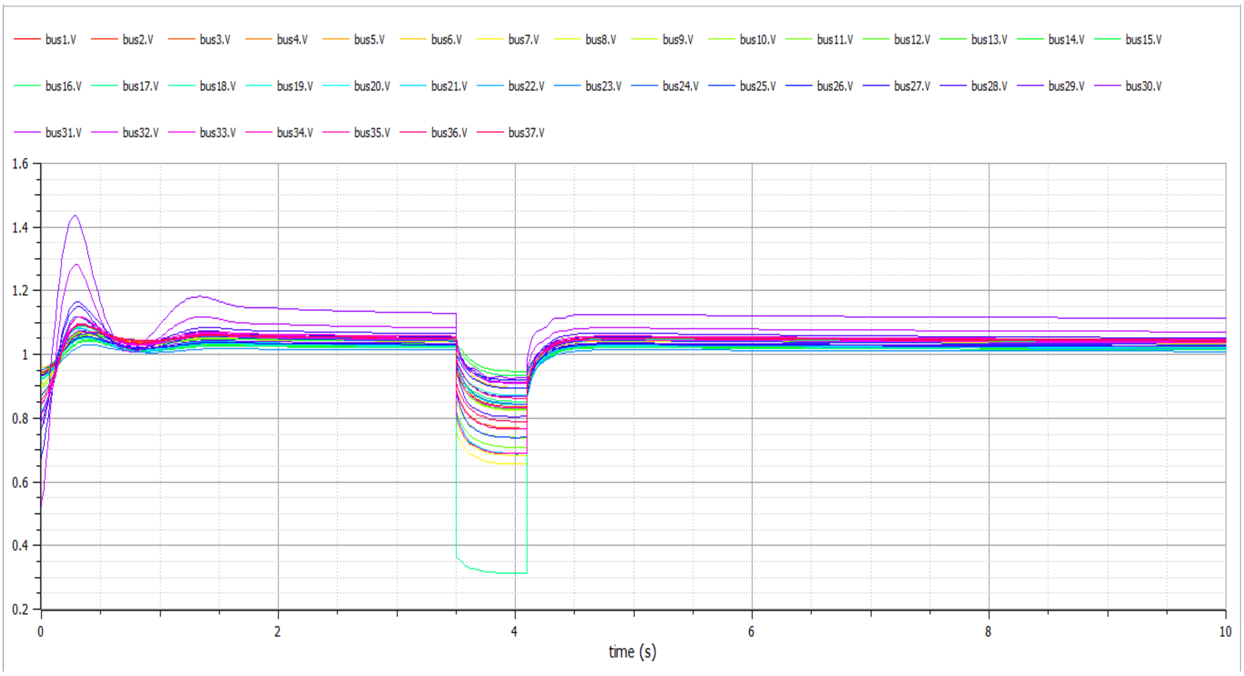

Figure 7.4 : All 37 buses voltage Profile Under Fault

7.2.2 Active Power Response of Generators

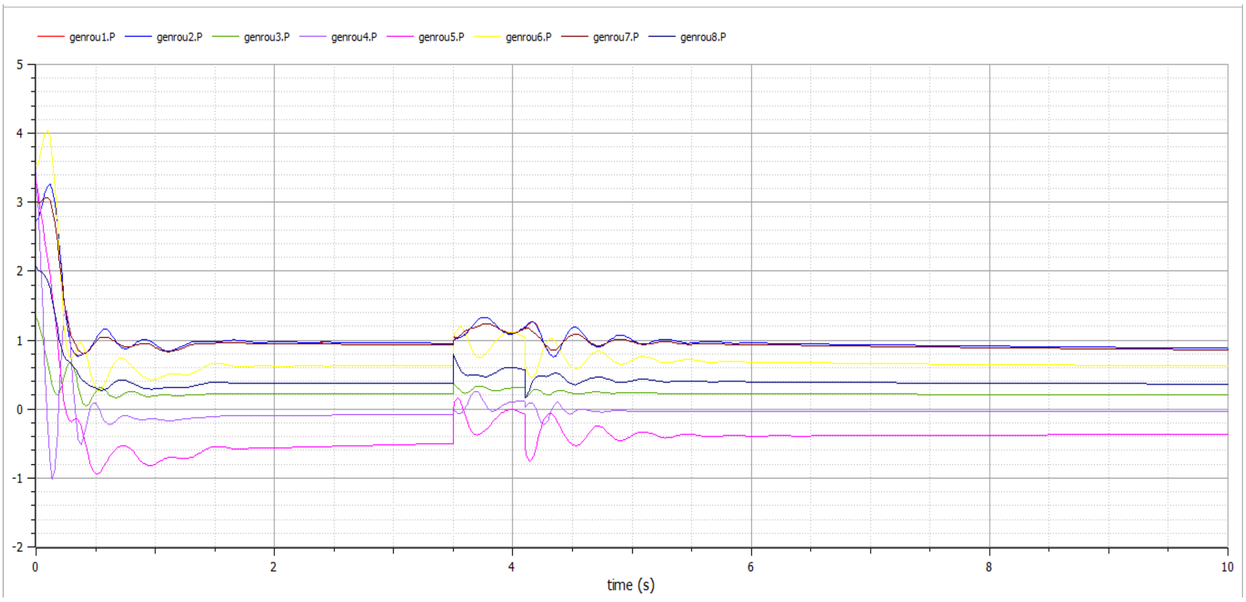

Figure 7.5 : Active Power Response of Generators Under Fault

7.2.3 Reactive Power Response of Generators

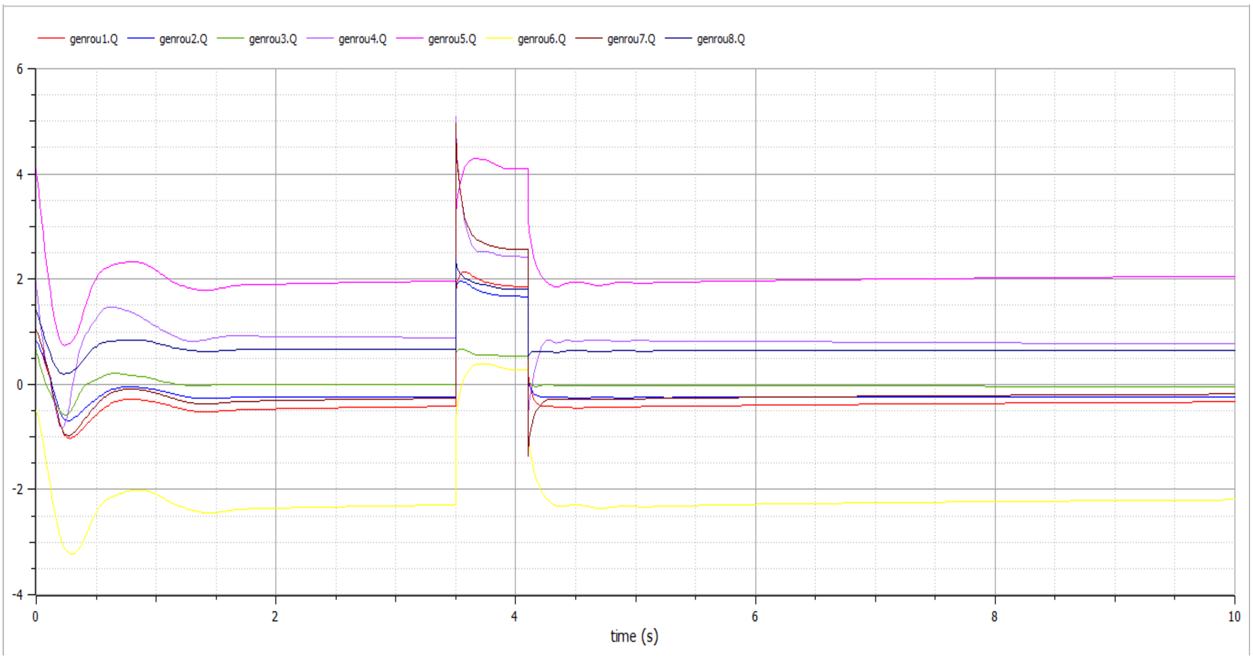

Figure 7.6 : Reactive Power Response of Generators Under Fault

7.2.4 Active Power Response of PV

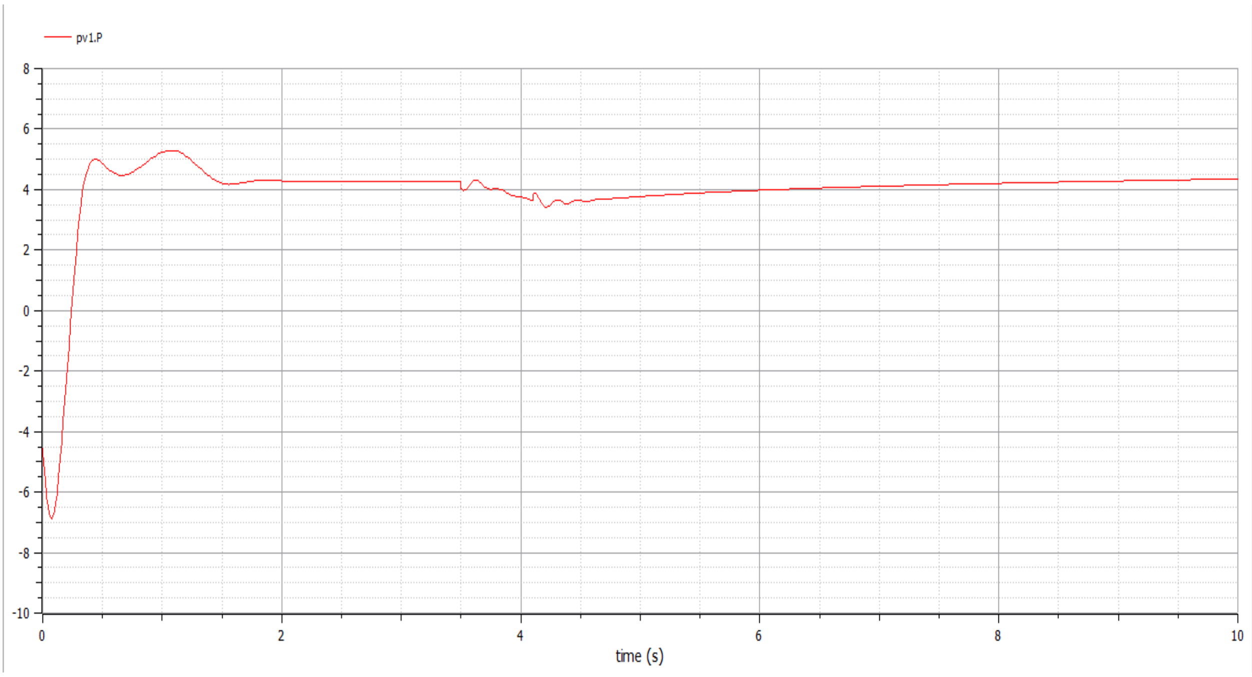

Figure 7.7 : Active Power Response of PV Under Fault

7.2.5 Reactive Power Response of PV

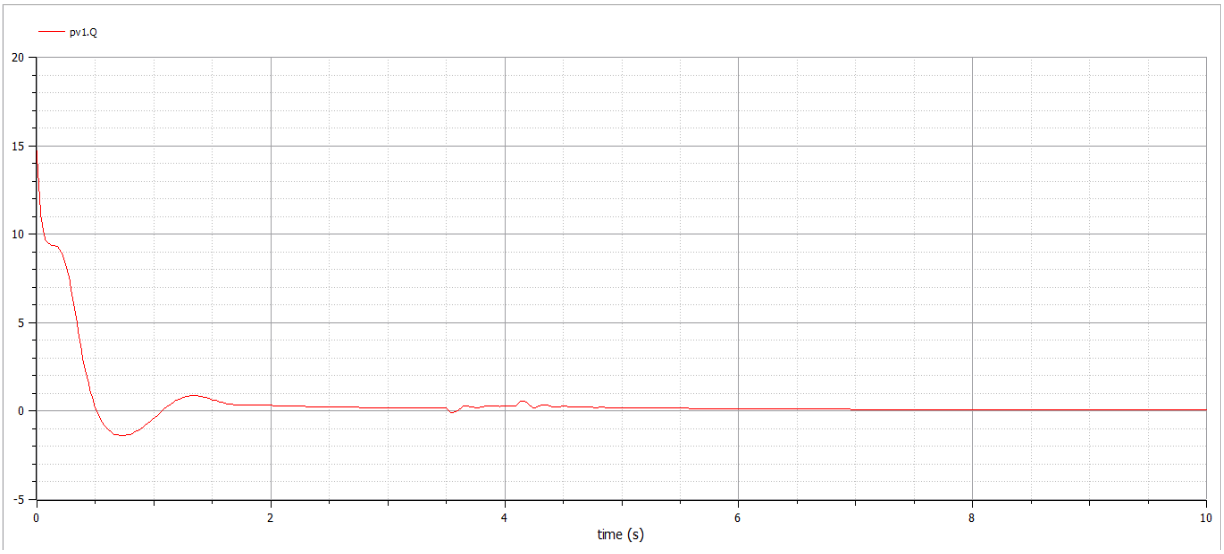

Figure 7.8 : Reactive Power Response of PV Under Fault

7.3 Case-3

This case is the simulation result of Model 6.3 (page 51).

7.3.1 Buses voltage Response

All buses Voltage

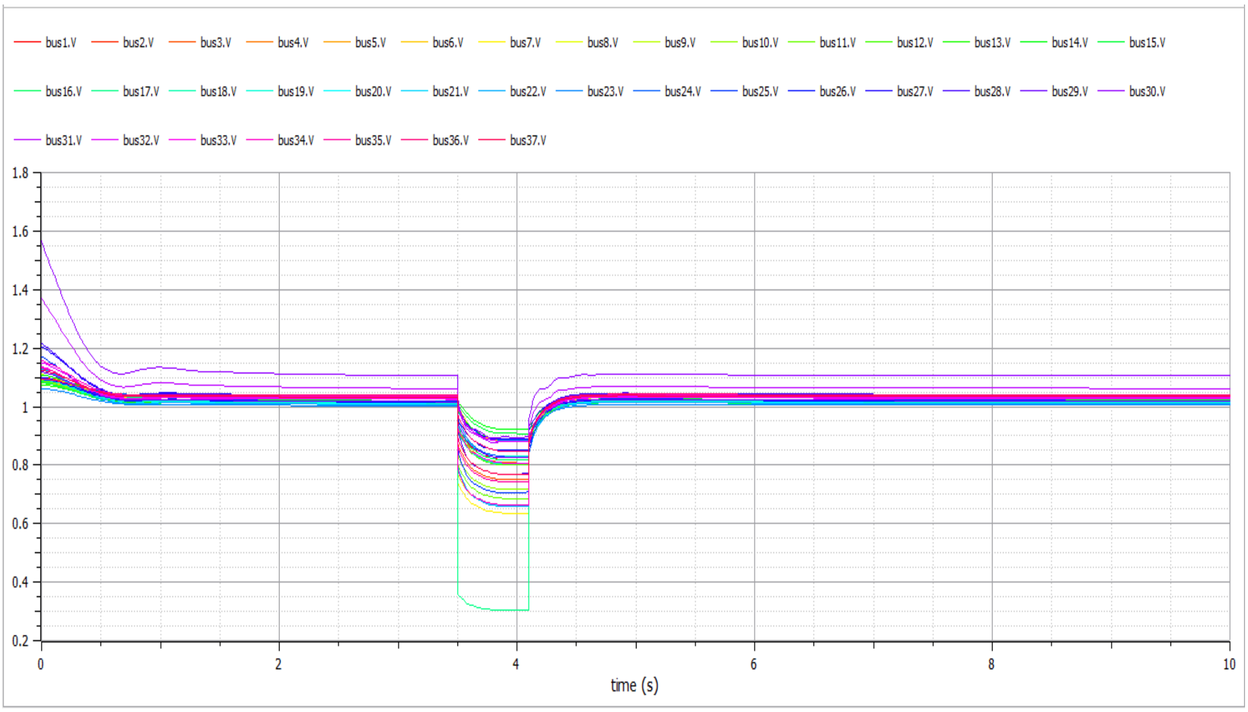

Figure 7.9 : All 37 buses voltage Profile Under Fault

Figure 7.9 shows that when applying fault on bus no 17, then voltage of all buses going dips. Voltage of faulty bus is got more dips compare to other buses. Duration of fault is 0.6 seconds from 3.5 sec to 4.1 sec after starting the simulation.
Fault is three phase symmetrical fault and the resistance of fault is 0 ohm (pu)
and reactance is 0.02015 ohm (pu). After the fault clearance of 4.1 seconds all bus voltages become steady state. The starting dips in voltage and occurs oscillation from 0 second to 1 second, is due to PV.

Slack Bus Voltage

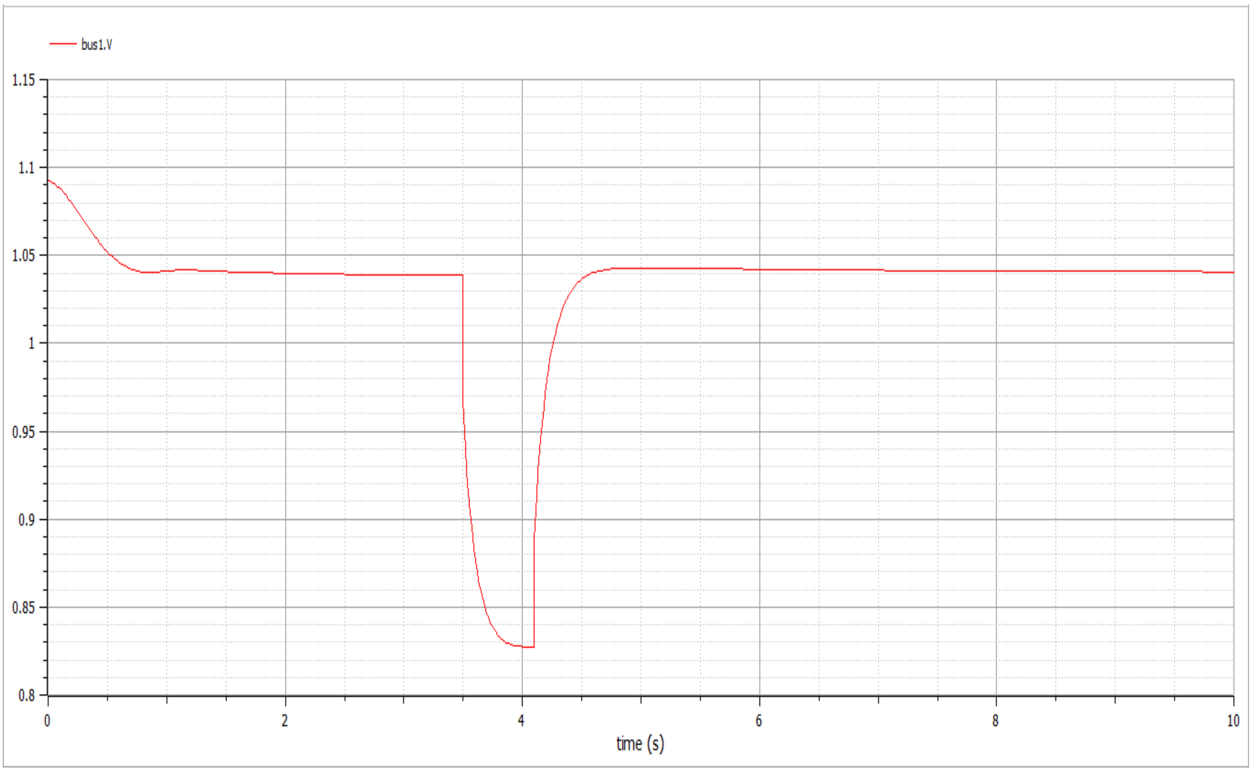

Figure 7.10 : Slack Bus (bus no 1) voltage Profile

Figure 7.10 shows that when simulation reaches at 3.5 second then voltage of slack bus goes to dips from 1.0388 to 0.8247. When fault is cleared after 4.1 second of simulation then bus voltage recovers at steady state and system further working on steady state. PV uses inverter for converting DC voltage to AC voltage and inverter does not produce reactive power. Hence the voltage dips in starting simulation occurs for 0 to 1 second.

Fault Bus Voltage

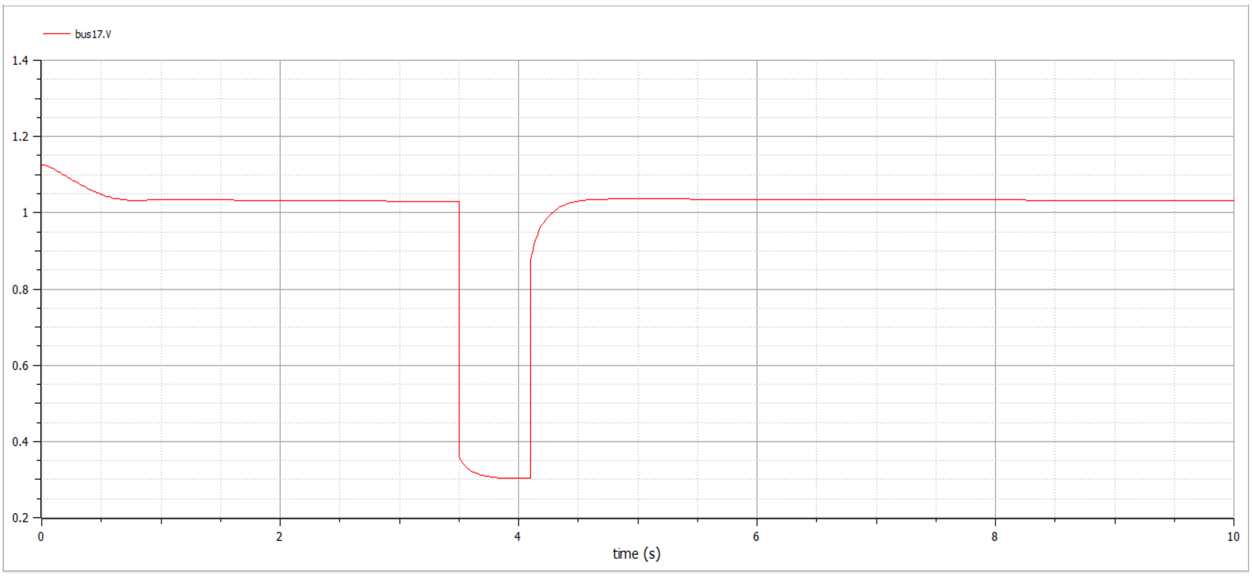

Figure 7.11 : Fault Bus (bus no 17) voltage Profile

Wind Turbine Generator Bus Voltage

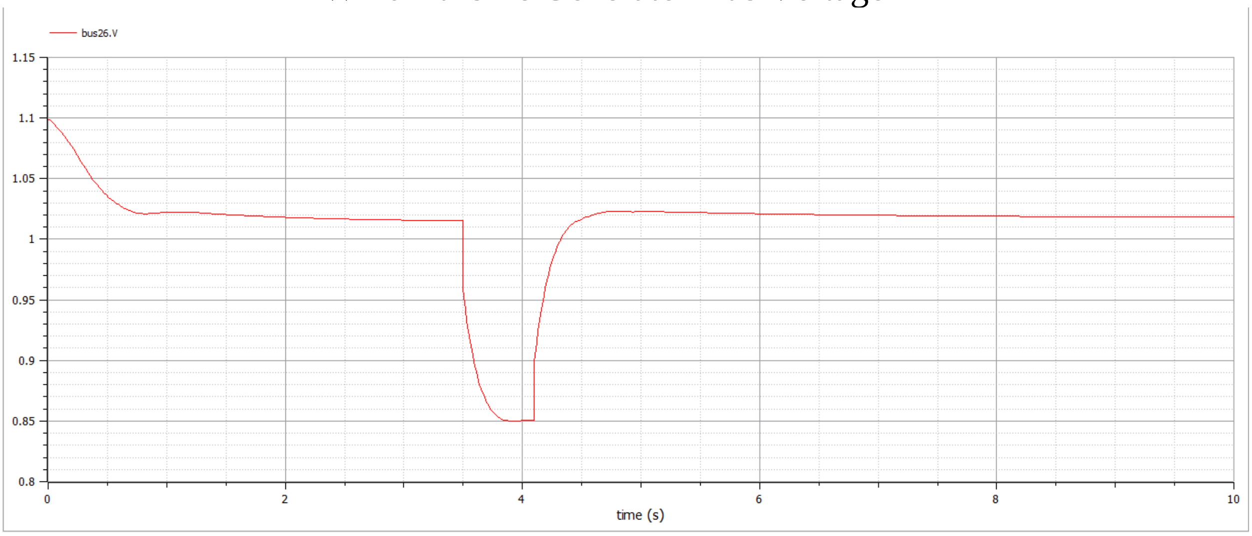

Figure 7.12 : Wind Turbine Generator Bus (bus no 26) voltage Profile

Figure 7.11 and 7.12 shows that the voltage profile of fault bus (bus no 17) and wind turbine generator bus (bus no 26) respectively. In this figure we see that at starting of simulation bus voltage drops instantly due to PV connected on bus no 30. After 1 second voltage goes to steady state. At 3.5 second when fault occurs, fault bus voltage dips from 1.0303 to 0.3034 pu and WTGs bus voltage dips from 1.0153 to 0.8507 pu. After clearance of fault voltage of both buses recovers to steady state.

Photovoltaic bus voltage

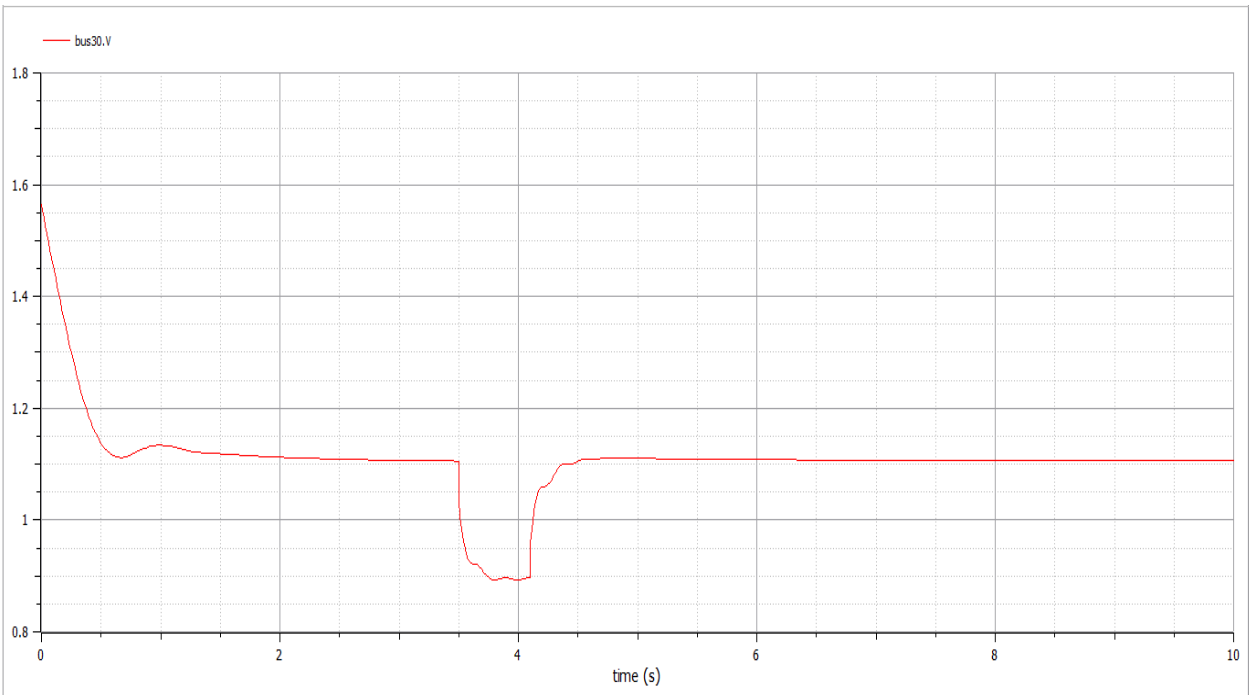

Figure 7.13 : Photovoltaic Bus (bus no 30) voltage Profile

In figure 7.13 instantaneous voltage drop from 1.55 to 1.11 pu and some oscillation in starting voltage is due to PV. Photovoltaic cell generates DC supply which converted to AC through inverter an we know that inverter supply only active power. Due to absence of reactive power voltage drops instantly and then recover steady state. So staring voltage drop in simulation occurs. Second voltage drop in figure 7.6 is due to fault from 3.5 to 4.1 second and after the clearance of fault some oscillation present for 0.5 seconds and then stayed at steady state.

Bus Voltage Magnitude after Simulation

Bus No	Voltage Magnitude (pu)
1	1.04072
2	1.03712
3	1.03802
4	1.03331
5	1.04072
6	1.03957
7	1.03111
8	1.02745

9	1.03235
10	1.01653
11	1.01390
12	1.01330
13	1.01437
14	1.03407
15	1.02211
16	1.00957
17	1.03263
18	1.01643
19	1.01409
20	1.01049
21	1.01817
22	1.00919
23	1.00465
24	1.04072
25	1.02014
26	1.01817
27	1.03997
28	1.03955
29	1.01942
30	1.10630
31	1.06210
32	1.03028
33	1.02718
34	1.03781
35	1.03434
36	1.04023
37	1.03434

Table 7.1 : Bus Voltage Magnitude After Simulation

7.3.2 Generator Response

- GENROU Active Power Response After Fault

Figure 7.7 & 7.8 shows that during the fault generator electrical power output suddenly increase and then decreases to a low value 0.8352 pu . The difference between the mechanical input power and electrical output power causes an increase in the rotor speed and therefore the rotor starts to accelerate and oscillation starts in output active power. After the fault is cleared it oscillate sometime and then will be constant. Figure 7.8 shows all generators active power response.

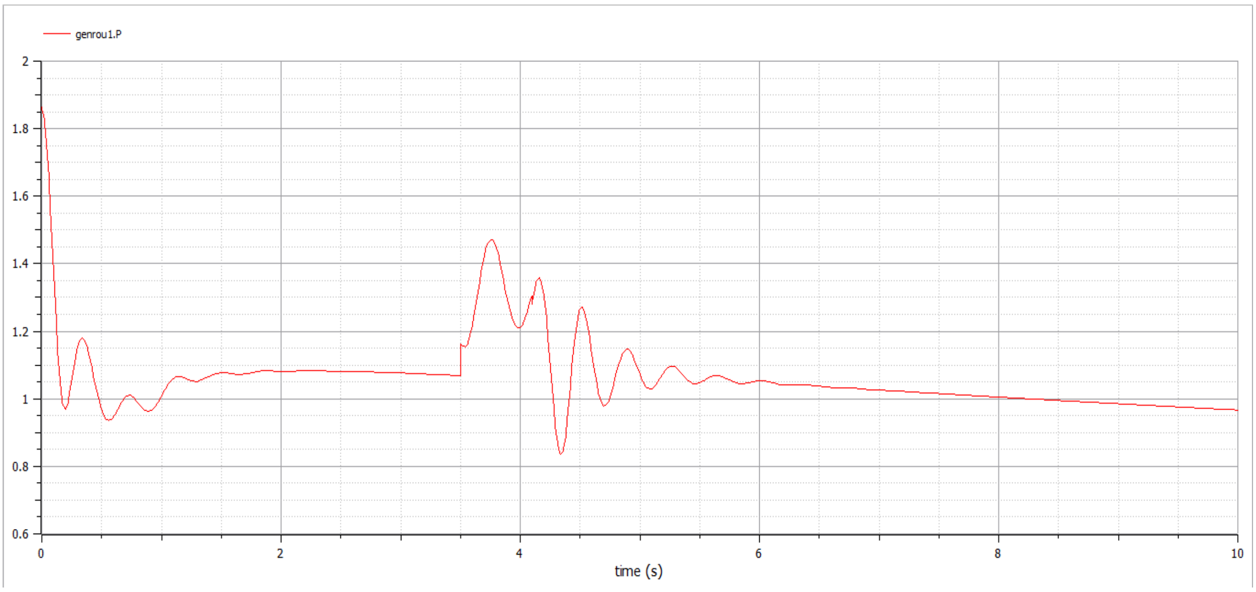

Figure 7.14 : Generator 1 (genrou 1) Active Power Response After Fault

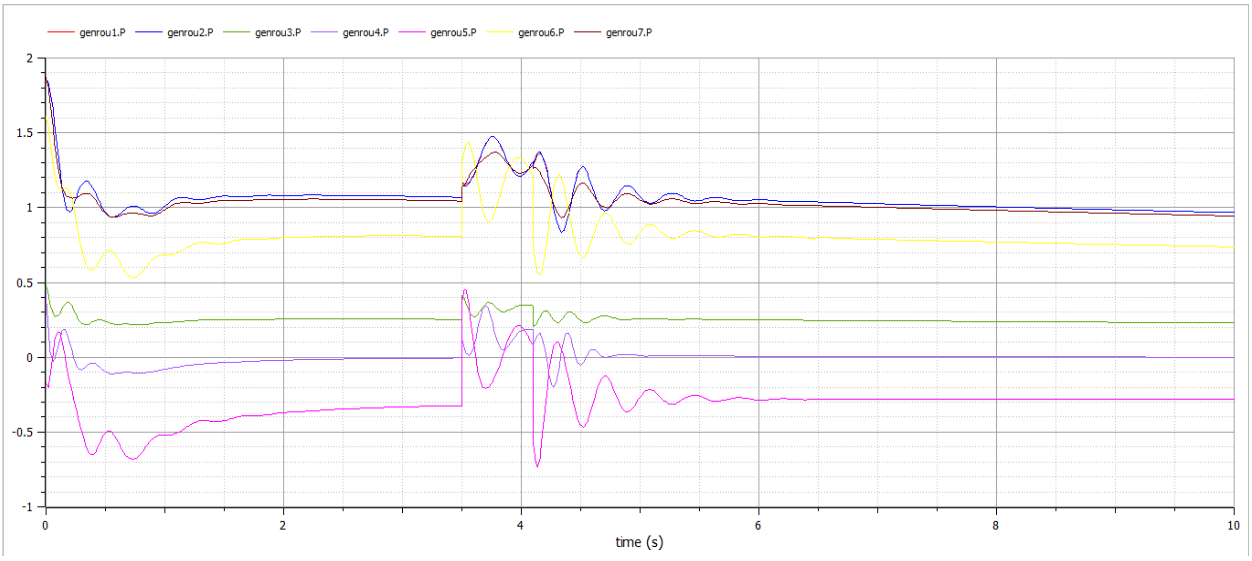

Figure 7.15 : All Generators Active Power Response After Fault

- GENROU Reactive Power Response After Fault

The reactive power outputs from selected generators (genrou 1) are shown in figure 7.9. Before the fault occurs, all genrou was injecting reactive power to the grid approximately steady state. During the fault, the rotor speed increases, giving a larger negative slip. This is because the electric power has decreased to almost zero whereas the mechanical power is assumed to be the same. As a result, prime mover decreased the mechanical power with the help of governor. During the fault, we can see that all generator units provide reactive power support to the grid. Figure 7.10 shows all generator reactive power provided to grid before and after fault.

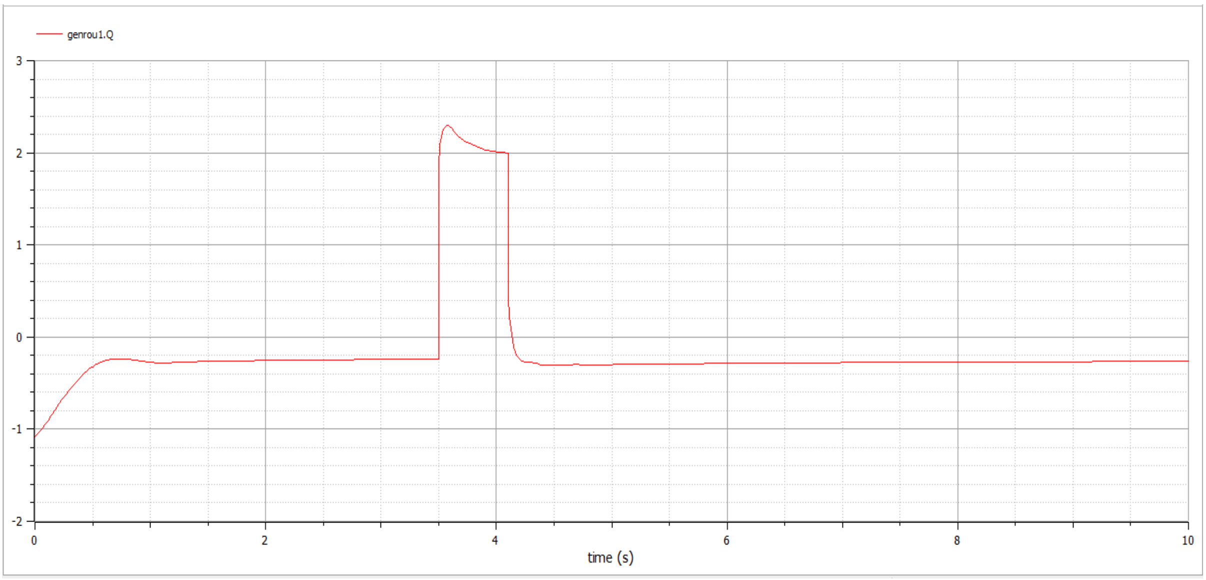

Figure 7.16 : Generator 1 (genrou 1) Reactive Power Response After Fault

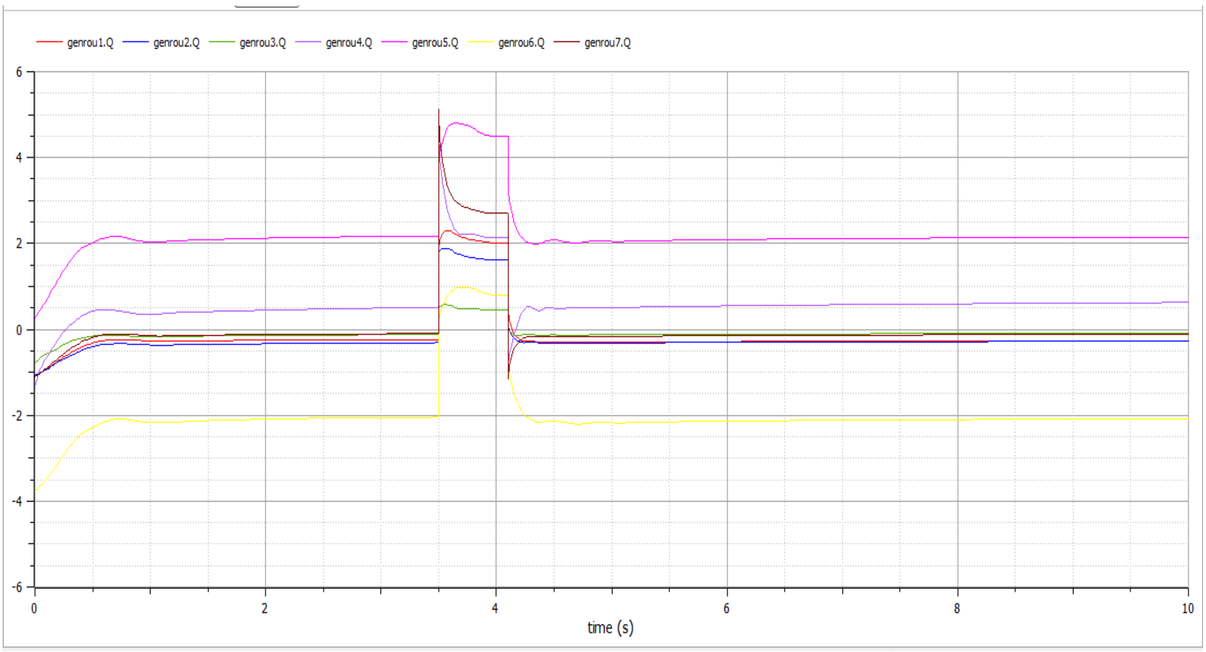

Figure 7.17 : All Generators Reactive Power Response After Fault

7.3.3 Wind Turbine Generator Response

➢ WTG Active Power Response After Fault

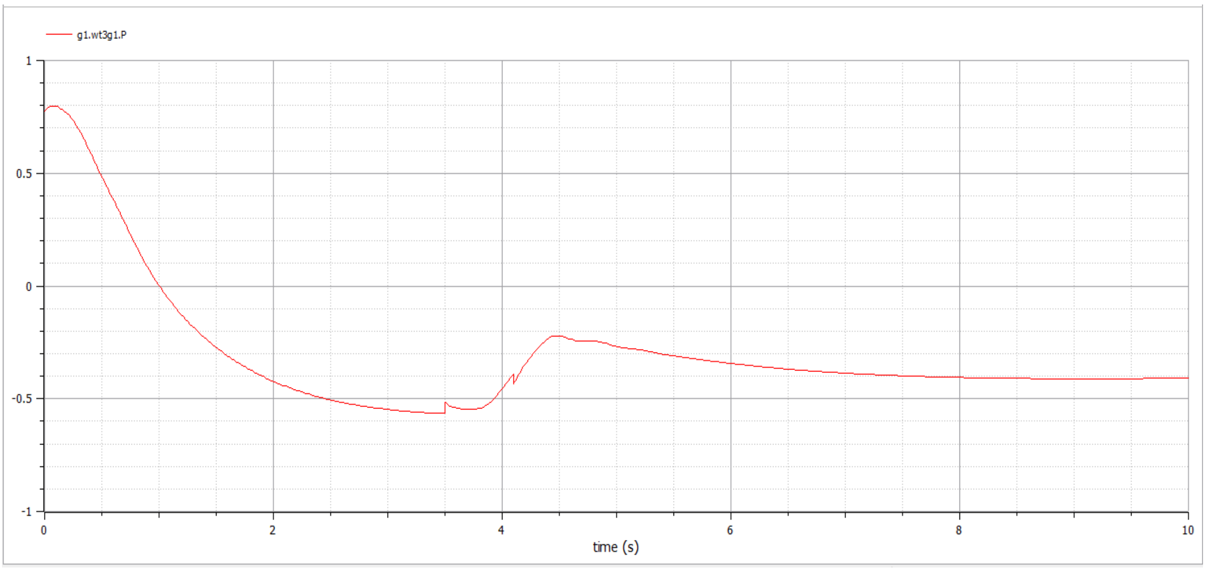

Figure 7.18 : Active Power Response of WTG After Fault

➢ WTG Reactive Power Response After Fault

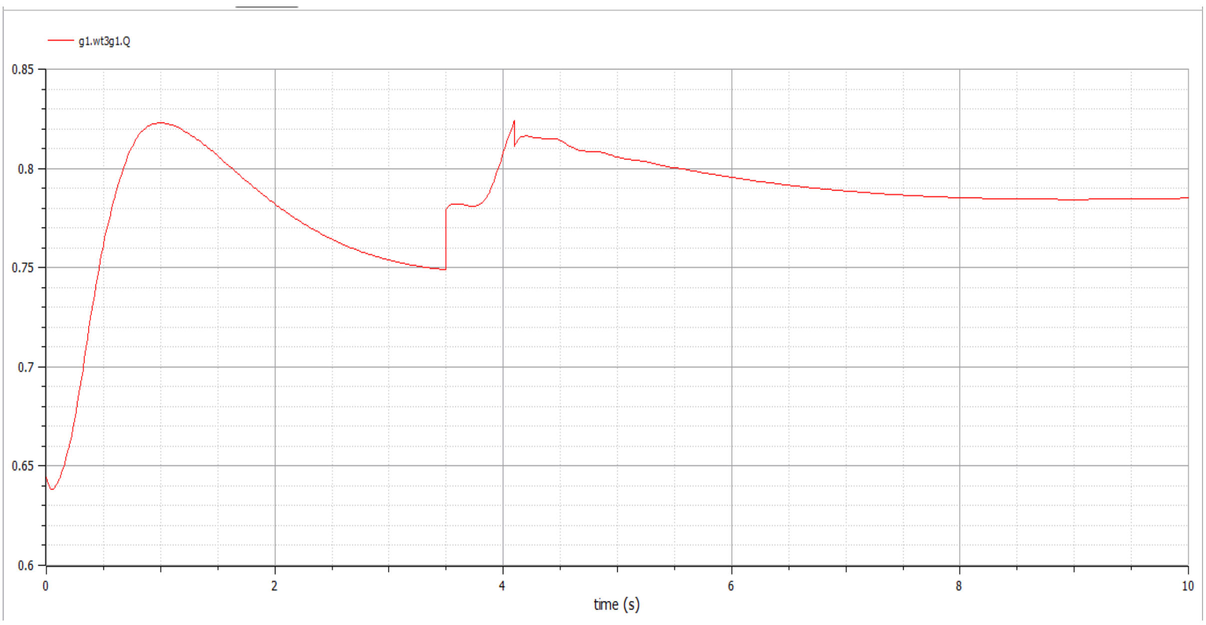

Figure 7.19 : Reactive Power Response of WTG After Fault

7.3.4 Photovoltaic (PV) Response

➢ PV Active Power Response After Fault

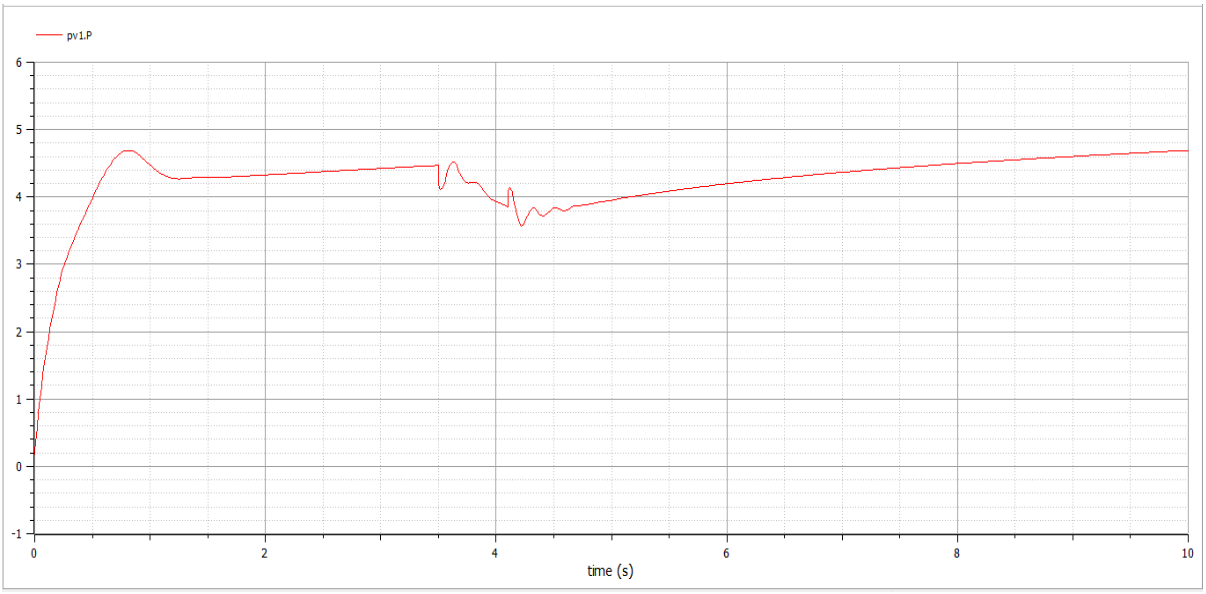

Figure 7.20 : PV Active Power Response After Fault

➢ PV Reactive Power Response After Fault

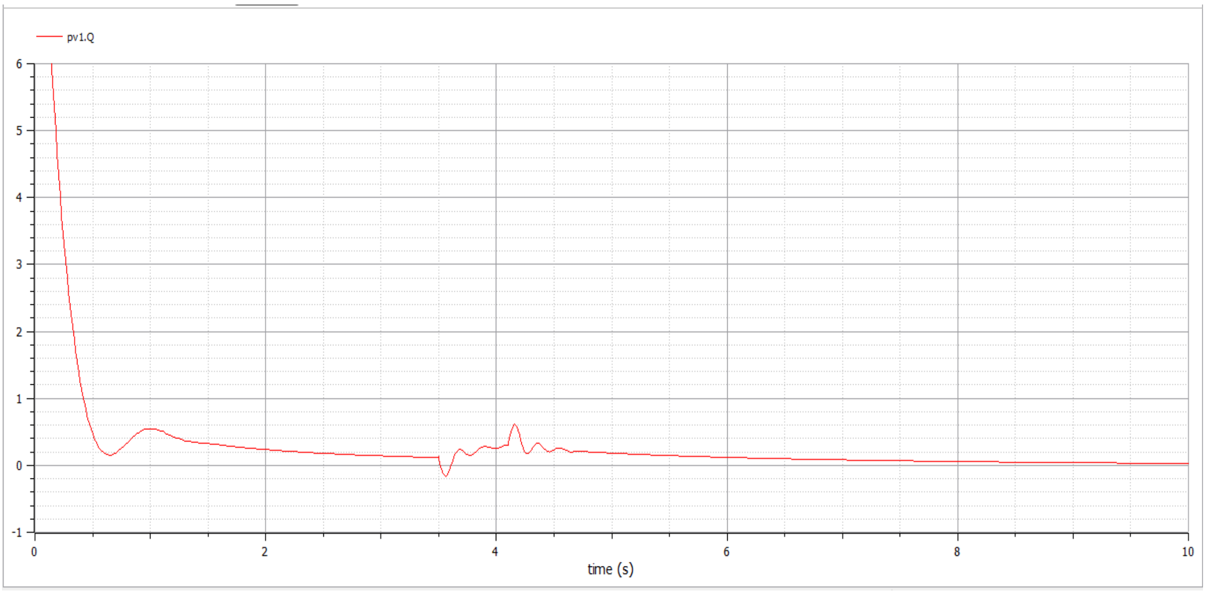

Figure 7.21 : PV Reactive Power Response After Fault

Chapter 8

Conclusion

The modeling of 37-bus model in OpenModelica is basically renewable energy integration. It represents the system behavior before and after the fault occurs at 17th Bus. WTG and PV voltage profile, active power and reactive power response mentioned in result. Some irrelevant behavior of reactive power of WTG and PV is due to using inverter in grid connected PV module because inverter cannot produce required reactive power. The voltage of all buses recovers after the fault clearing. The voltage profile of the buses indicates that the system can be brought back to stable operating condition even faster by adding additional controls such as power system stabilizer (PSS) and automatic voltage regulator (AVR).

Reference

1. Power System Analysis, www.nptel.ac.in.
2. Fast Decupled Method of Load Flow Solution, https://www.engineeringenotes.com/electrical-engineering/power-flow/fast-decoupled-method-to-solve-power-flow-problem-electrical-engineering
3. 'Renewable and Sustainable Energy Reviews' www.elsevier.com.
4. 'Testing and model validation of round rotor synchronous generator (GENROU)' by 'Saifal Talpur', Auckland University of Technology, New Zealand. www.elsevier.com
5. Wind Grid Code, www.kostt.com.
6. WT3 – Generic Wind Model, www.esig.energy..
7. Generic Models (Individual Turbines), www.esig.energy.
8. Design of grid-connected photovoltaic inverter digital control module, www.ijird.com.
9. Analysis of Grid-Connected Inverter for PV Generation, Proceedings of the 2nd International Conference on Computer Science and Electronics Engineering (ICCSEE 2013).
10. 37 bus system, 'Power System Analysis and Design' by J. Duncan Glover and Mulukutla S. Sarma .
11. 37 bus system, www.al-rooomi.org